Persisting impact of historical mining activity to metal (Pb, Zn, Cd, Tl, Hg) and metalloid (As, Sb) enrichment in sediments of the Gardon River, Southern France

Eleonore Resongles, Corinne Casiot, Remi Freydier, Laurent Dezileau, Jerome Viers, Francoise Elbaz-Poulichet

Persisting impact of historical mining activity to metal (Pb, Zn, Cd, Tl, Hg) and metalloid (As, Sb) enrichment in sediments of the Gardon River, Southern France

Eléonore Resongles[a]*, Corinne Casiot[a], Rémi Freydier[a], Laurent Dezileau[b], Jérôme Viers[c] and Françoise Elbaz-Poulichet[a]

[a] HydroSciences UMR 5569, CNRS, Universités Montpellier I & II, IRD, Place Eugène Bataillon, CC MSE, 34095 Montpellier Cedex 5, France

[b] Géosciences UMR 5243, CNRS, Universités Montpellier II, Place Eugène Bataillon, CC 60, 34095 Montpellier Cedex 5, France

[c] Géosciences Environnement Toulouse UMR 5563, Université Paul Sabatier, CNRS, IRD, 14 Avenue Edouard Belin, 31400 Toulouse, France

Abstract

In this study, we assessed past and present influence of ancient mining activity on metal(loid) enrichment in sediments of a former mining watershed (Gardon River, SE France), that is now industrialized and urbanized. A sedimentary archive and current sediments were characterized combining geochemical analyses, zinc isotopic analyses and sequential extractions. The archive was used to establish local geochemical background and recorded (i) increasing enrichment factors (EF) for Pb, Zn, Cd, Tl, Hg, As and Sb throughout the industrial era, (ii) a contamination peak in 1976 attributed to a tailings dam failure, and (iii) current levels in 2002 and 2011 similar to those of 1969, except for Sb and Hg, reflecting a persisting contamination pattern. Inter-element relationships and spatial distribution of EF values of current sediments throughout the watershed suggested that both ancient and current contamination had a common origin for Pb, Zn, Cd, Tl and As related to the exploitation of Pb/Zn mineralization while old Sb mines and coal extraction area were the main sources for Sb and Hg respectively. This prevailing mining origin was reflected for Zn by a relatively uniform isotopic composition at $\delta^{66}Zn$ = 0.23±0.03‰, although slight decrease from 0.23‰ to 0.18‰ was recorded from upstream to downstream sites along the river course in relation with the contribution of the lighter $\delta^{66}Zn$ signature (~0.08‰) of acid mine drainage impacted tributaries. Results from sequential extractions revealed that the potential mobility of the studied metal(loid)s varied in the order Sb<Tl≈As<Zn<Pb<Cd, with an increase of the mobile pool for Cd, Pb, Zn and to a lesser extent for As and Tl associated to increased enrichment. Altogether, these results tend to demonstrate that ancient mining activity still contributes to metal enrichment in the sediments of the Gardon River and that some of these metals may be mobilized toward the water compartment.

Keywords

Mining-affected river; Metal and metalloid; Sedimentary archive; Zinc isotopes; Sequential extraction

1 Introduction

Mining activity is one of the most important sources of harmful metals (Pb, Zn, Cd, Tl, Hg) and metalloids (As, Sb) to rivers (Byrne et al., 2012; Hudson-Edwards, 2003; Johnson and Hallberg, 2005; Nriagu and Pacyna, 1988; Schwarzenbach et al., 2010). Damage to surface water ecosystems has been recognized in many areas in the United States (Caruso et al., 2008; Cherry et al., 2001; Peplow and Edmonds, 2005), the United Kingdom (Gray, 1997; Jarvis and Younger, 1997), France (Audry et al., 2004a; Monna et al., 2011), Spain (Bonilla-Valverde et al., 2004), with dramatic accidents such as those of Aznalcollar in Spain (Grimalt et al., 1999) or Maramureş County in Romania (Macklin et al., 2003). A peculiarity of mining related pollution is that tailings, waste piles, ochre sediments and contaminated floodplains continue acting as secondary sources for pollutants to downstream watershed throughout hundreds of years after the mine closure (Byrne et al., 2012; Johnson and Hallberg, 2005; MacKenzie and Pulford, 2002; Macklin et al., 1997; Younger and Wolkersdorfer, 2004). Furthermore, the extent of contamination is not strictly limited to the vicinity of mines; contaminated material (i.e. tailings, contaminated river bed and floodplain sediments) may be physically remobilized in high flow conditions (Hudson-Edwards, 2003; Hudson-Edwards et al., 1997; Miller, 1997; Moore and Langner, 2012), thus dispersing pollutants over hundreds of kilometers away from historical mining sites (Grosbois et al., 2012; Moore and Luoma, 1990; Salomons, 1995).

In Europe, the Water Framework Directive (2000/60/EC) aimed to achieve good ecological status of water bodies by 2015 and has reinforced the need for management of streams and rivers at the catchment scale (Kimball and Runkel, 2009; Mayes et al., 2009; Mighanetara et al., 2009). While metal discharges from industrial activities have decreased as a result of more stringent controls, pollution from historical mining persists and its relative contribution to anthropogenic emissions of metals and metalloids to downstream watersheds has become more important over recent years (Macklin et al., 2006). In the perspective of optimizing remediation strategies at the river basin scale, achieving maximum improvements of downstream water quality, it is essential to develop approaches allowing evaluation of the impact of abandoned mining sites on metal enrichment to downstream river systems and to distinguish metals from such sources from natural geochemical background and other anthropogenic (industrial, urban) point sources. In environmental studies, metal isotope geochemistry may be useful to complement traditional geochemical data to track metal sources and elucidate processes affecting their transport and fate in rivers (Cloquet et al.,

2008; Weiss et al., 2008). Zn has five stable isotopes, ^{64}Zn, ^{66}Zn, ^{67}Zn, ^{68}Zn, and ^{70}Zn, with average natural abundances of 48.63%, 27.90%, 4.10%, 18.75% and 0.62% respectively (Rosman and Taylor, 1998). Previous studies have reported Zn isotope variations (expressed as $\delta^{66}Zn$ unit) of 2.5‰ in terrestrial samples (Cloquet et al., 2006). In mining environments related studies, Zn isotopic composition of the main Zn-ore (sphalerite, ZnS) was shown to cover a large range of $\delta^{66}Zn$ from -0.17‰ to 0.64‰ with an average of +0.16±0.20‰ (Sonke et al., 2008). Borrok et al., (2008) reported $\delta^{66}Zn$ values between 0.02‰ and 0.46‰ for dissolved Zn in streams draining historic mining districts in the United States and Europe. Several physical and biogeochemical reactions including evaporation, inorganic and organic adsorption, diffusion and biological uptake can induce Zn isotope fractionation (Cloquet et al., 2008). Largest Zn isotopic variations are observed associated with smelting industry; atmospheric emissions are enriched in the lighter Zn isotopes while slag are enriched in the heavier Zn isotopes (Mattielli et al., 2009; Sivry et al., 2008; Sonke et al., 2008). The potential of Zn isotopes to track pollution sources has already been demonstrated in urban, mining and smelting impacted environments (Borrok et al., 2009; Chen et al., 2008, 2009; Dolgopolova et al., 2006; Mattielli et al., 2009; Sivry et al., 2008; Sonke et al., 2008; Thapalia et al., 2010).

In the present study, we investigated the impact of abandoned mines localized in the Cevennes Mountains to metal (Pb, Zn, Cd, Tl, Hg) and metalloid (As, Sb) enrichment in the sediments of the Gardon River watershed, which is a tributary of the Rhône River. The River Gardon catchment is around 2,000 km^2 with 180,000 people. Multiple mining sites are referenced on this catchment (BRGM, SIG Mines website; Vincent, 2006), including scattered metal mines (Pb, Zn, Ag, Sb) and a coal production district (La Grand-Combe). Besides, one mid-size town (Ales, 40,000 inhabitants) and a chemical and industrial center (Salindres) constitute other possible point sources of metals and metalloids to the watershed. The impact of ancient mining activity on global contamination of the watershed by metals and metalloids has never been evaluated (SMAGE des Gardons, 2011), although severe local pollution was evidenced in the vicinity of some of these mining sites (Casiot et al., 2009).

In this study, we propose a methodological framework allowing catchment-scale assessment of in-stream mining-related pollution. For this, a sedimentary archive was used to establish the natural geochemical background levels of metals and metalloids of the watershed and reconstruct a historical record of metal and metalloid enrichment. Enrichment factors were determined for current sediments of the Gardon River and for those of its main tributaries. Inter-element correlations and zinc isotope ratios were used to track the contribution of disused mining sites to sediment contamination. Geochemical associations of Pb, Zn, Cd, Tl,

As and Sb, evaluated using the BCR sequential extraction procedure, allowed assessment of the potential mobility of these contaminants in the sediments.

2 Material and methods

2.1 Study area

The Gardon River watershed is located at the southeast of the Massif Central Mountains in France. This tributary of the Rhône River is 144 km long and drains an area of 2,014 km². The watershed includes three main geological areas (1) Primary metamorphic (schists and micaschists) and igneous (granite) rocks in the upstream part of the watershed (Cevennes Mountains region), (2) Jurassic carbonate formations (limestone and dolomite) along the Cevennes Mountains boundary, (3) Cretaceous limestone formation (Gardon River gorges) and Quaternary alluvium deposits of the Rhône River in the downstream watershed (Figure 1a, BRGM, Info Terre website). In the area of Ales-La Grand-Combe, a graben filled with Tertiary detrital sediments represents the most important coalfield of the Cevennes Mountains. Hydrologically, the Gardon River is characterized by high seasonal variability including severe low water during summer and extreme floods with peak reaching 100 times the average discharge mainly in autumn.

The upstream watershed drains many disused mining sites (Figure 1b, Table 1). Mining activity began on the Gardon River watershed during Roman Times for Ag and Middle Ages for Ag, Pb and coal (Rolley website; Vincent, 2006). The large-scale production started from the middle of the 19th century and declined after 1960. During this period, we estimated that about 4Mt of pyrite, 85,000t of Zn, 50,000t of Pb and 2,570t of Sb were produced on the Gardon River watershed leaving several millions of tons of wastes close to ore extraction and processing sites (BRGM, SIG Mines website). Exploited ores were in the form of sulfide minerals (galena and argentiferous galena for Pb and Ag, sphalerite for Zn and stibnite for Sb). These minerals were associated to other unexploited sulfide minerals such as pyrite and marcasite (FeS_2), tetraedrite ($Cu_{12}Sb_4S_{13}$), pyrargyrite (Ag_3SbS_3) and proustite (Ag_3AsS_3) described for the Carnoulès mine drained by the Amous River (AF9) (Alkaaby, 1986). On the Gardon of Anduze River subwatershed, the most important Pb/Zn mining districts were those of Carnoulès and Pallières, drained respectively by the Amous River (AF9) and the Ourne and Aiguesmortes Rivers (AF8 and AF10). Antimony mines are localized on the upstream subwatershed of the Gardon of Ales River and they are drained by the Ravin des Bernes and

the Richaldon Rivers (AF1 and AF2). Downstream, in the area of Ales-La Grand-Combe, coal has been exploited intensively. Finally, the Grabieux River (AF4), the Alzon River (AF5) and the Avène River (AF6), on the Gardon of Ales River subwatershed, drain old Pb/Zn/pyrite mining sites. Most of these tributaries are impacted by metal and metalloid contamination downstream from these mining sites (SMAGE des Gardons, 2011). Pollution from the abandoned Pb/Zn mine of Carnoulès was already mentioned in 1970 (Michard and Faucherre, 1970) and to date, the Amous River remains highly impacted (Casiot et al., 2009). In addition to the extractive activity, three smelters have been in activity on the watershed; a Zn smelter at La Grand-Combe town with a period of activity from 1846 to 1899 (Ministère de la Culture) and two small Sb smelters located on the upstream Gardon of Ales River near Sb mining sites which had worked from 1822 to 1858 and from 1896 to 1951 (BRGM, BASIAS website).

Nowadays, the chemical industrial center of Salindres and the urban area of Ales (40,000 inhabitants) can also contribute to metals and metalloids enrichment of the Gardon River. The Avene River (AF 6) is both impacted by industrial and mining discharges. According to the French Water Agency, 27kg d^{-1} of metals and metalloids were released in 2007 in the Gardon River by industrial activities and urban wastewater treatment plants (SMAGE des Gardons, 2011).

2.2 Sampling

2.2.1 Sedimentary archive

The sedimentary archive (GE) was sampled in March 2010 in the downstream part of the watershed (Figure 1b), in a zone of canyon. This flooding terrace, situated between 6.20 and 9.50 m above the riverbed level, was formed by the accumulation of extreme flood deposits (Dezileau et al., 2013; Dezileau et al., in review). These flood events have resulted in one sedimentary layer each. The terrace was composed of 20 layers corresponding to 20 extreme flood events; these layers were identified in the field through a close inspection of deposition breaks and/or indicators of surficial exposure (e.g. presence of a paleosol, clay layers at the top of a unit, detection of erosional surfaces, bioturbation features, angular clast layers deposits in local alcove or slope materials accumulation between flood events, fireplaces and anthropogenic occupation layers between flood events). Sedimentary layers were numbered from the bottom to the top of the terrace and named GE1 to GE20. Samples were excavated directly from the terrace using a Teflon spatula and collected in PP-jars. Sieving was not

necessary because all particles were finer than 2mm. Then, samples were air-dried, crushed in an agate mortar and homogenized before further processing. Dating of sedimentary layers was based on an original method using a multi-dating approach described in Dezileau et al. (in review). Radionuclide analyses (^{210}Pb, ^{137}Cs) and geochemical analyses (total Pb) were used to determine age controls. Maximum ^{137}Cs activity in layers GE17 and GE18 was associated to the maximum atmospheric emission in the mid-1960s. ^{210}Pb activity results indicated that layers GE15 to GE20 were deposited after the end-1930s. Pb concentration was constant in layers GE1 to GE9 and increased from the layer GE10 showing that layers GE1 to GE9 dated back the beginning of large-scale mining activity on the watershed around 1870. These age controls were combined with the continuous record of Gardon River flow since 1890, the combined records allow to assign ages to the most recent layers, from GE9 to GE20 (Dezileau et al., 2013; Dezileau et al., in review).

2.2.2 Current stream sediments

Active stream sediments in contact with stream water were studied; this sampling medium integrates both natural geochemical characteristics and recent anthropogenic contamination of the whole watershed upstream from the sampling station over time (Ettler et al., 2006; Gosar and Miler, 2011). Six surveys were carried out from 2010 to 2012 in low flow and high flow conditions; stream sediments were sampled on the upper part of the watershed, along the Gardon River and on the tributaries of interest i.e. main tributaries and tributaries impacted by mining, industrial or urban activities. The location of the sampling stations is shown in Figure 1b. Stream sediments were collected in PP-jars using a Teflon spatula, in the first centimeter of the riverbed surface, as far as possible from the riverbank. Back in the laboratory, the sediment samples were sieved <2 mm, freeze-dried and powdered in an agate mortar.

2.3 Sample preparation

2.3.1 Bulk mineralization

Total digestion of sediment samples was carried out in a clean room. All material was acid-cleaned before use; reagents were Merck Suprapur quality. For each set of samples, method blanks and international certified reference materials digestion (Stream sediments LGC6189 from United Kingdom Accreditation Service and NCS DC70317 from LGC Standards) were performed. About 100 mg of sediment samples were digested in closed Teflon reactors on hot-plates at 95 °C for 24 h successively with (1) H_2O_2 35% (2) a 4:3:0.13 mL concentrated

HNO_3-HF-$HClO_4$ mixture and (3) a 1:3 mL concentrated HNO_3-HCl mixture (aqua regia). Samples were cooled and evaporated to dryness between each step and at the end of the procedure. Samples were brought to 30mL using 3mL HNO_3 and double deionized water (Milli-Q®). Finally samples were filtered to remove possible residues.

2.3.2 Chemical purification for zinc isotopic analyses

Zn isotopic analyses were carried out on the sedimentary archive samples and on the current sediments samples of the November 2011 sampling campaign. Digested solution aliquots containing approximately 1000ng of Zn were used for Zn separation and isotopic measurement. Zn was separated from the matrix elements by ion chromatography using AG1-MP1 anion-exchange resin (Biorad) and the elution sequence from Maréchal et al. (1999). The protocol was repeated twice to ensure Zn purity. The total procedural blank of ≈15ng was negligible compared to the amount of Zn in samples (1000ng). Column yields were checked for each sample by ICP-MS, X Series II (Thermo Fisher Scientific) and found to be >96%. After the purification, samples were evaporated to dryness at 60°C. Then samples were taken up in 3.3mL of HNO_3 0.05N and doped with a Cu standard (Cu NIST-SRM 976); final Zn and Cu concentrations were 300ng.g^{-1}.

2.3.3 Selective sequential extraction procedure

Total metal and metalloid concentrations are insufficient to evaluate the potential mobility of these contaminants in stream sediments. Therefore, selective sequential extractions were performed to characterize the distribution of Pb, Zn, Cd, Tl, As and Sb in sediment samples. Selected samples from the sedimentary archive and current sediments were subjected to a four-step sequential extraction procedure using the standardized method of the European Community Bureau of Reference (BCR) described by Rauret et al. (1999). Metals and metalloids were extracted into the following four operationally defined fractions: exchangeable and carbonate fraction (F1), reducible fraction (bound to Fe and Mn oxides/hydroxydes) (F2), oxidisable fraction (bound to organic matter and sulfides) (F3) and residual fraction (F4). The fraction F4 was determined using a procedure of mineralization assisted by microwaves; 100mg of the residual solid was digested by a 2:4 mL concentrated HF:HNO_3 mixture. Then samples were cooled, evaporated to dryness and brought to 30mL using 3mL HNO3 and double deionized water (Milli-Q®).

2.4 Analyses

Metal (Pb, Zn, Cd, Tl), metalloid (As, Sb) and Al concentrations in sediments (total and selective extractions) were determined after an adequate dilution using an ICP-MS, X Series II (Thermo Fisher Scientific) equipped with a CCT (Collision Cell Technology) chamber. The quality of analytical methods was checked by analyzing international certified reference waters (SLRS-5, NIST1643e) and was generally better than 5% relative to the certified values. Analytical error (relative standard deviation) was better than 5% for concentrations ten times higher than the detection limits. Accuracy was within 10% of the certified values for method standards (Stream sediments LGC6189 from United Kingdom Accreditation Service and NCS DC70317 from LGC Standards, n=7) with recoveries of 95±7% for As, 100±4% for Cd, 95±7% for Pb, 101±4% for Sb, 95±4% for Tl and 100±10% for Zn except for Al for which recovery was 86±6%.

For total Hg determination, about 0.1g of crushed air-dried sediments was analyzed using a Direct Mercury Analyzer (DMA-80 Milestone) following the 7473 EPA standard method. To ensure analytical results precision, a certified reference material (Stream Sediment NCS DC70317 from LGC Standards) was analyzed every ten samples, accuracy was better than 10% for certified Hg concentration (34.4±3.3 $ng.g^{-1}$, n=12). The procedural blank represents at most 2.7% of Hg measured in samples.

Zn isotopic analyses were performed on a multiple-collector inductively coupled plasma mass spectrometer (MC-ICP-MS) during several sessions at GET (Toulouse, France) on a Neptune (Thermo-Scientific) and at ENS Lyon (Lyon, France) on a Nu Plasma 500 HR. Each sample was analyzed three times and was bracketed with the Lyon reference solution JMC 3-0749-L. Zn isotopes (^{64}Zn, ^{66}Zn, ^{67}Zn, ^{68}Zn), Cu isotopes (^{63}Cu, ^{65}Cu) and Ni isotope (^{62}Ni) were monitored simultaneously. Measurements of ^{62}Ni signal allowed correcting the possible isobaric interference of ^{64}Ni on ^{64}Zn. Instrumental mass bias was corrected using Cu internal standard NIST-SRM 976 and the exponential law coupled with the method of sample-standard bracketing (Maréchal et al., 1999). Zn isotopic results are given as $\delta^{66}Zn$ notation (in units of ‰), $\delta^{66}Zn$ is the deviation relative to a standard, the Lyon reference solution JMC 3-0749-L :

$$\delta^{66}Zn = \left(\frac{\left(^{66}Zn/^{64}Zn\right)_{sample}}{\left(^{66}Zn/^{64}Zn\right)_{reference}} - 1 \right) \times 1000$$

Results are also given normalized to the standard IRMM-3702 calibrated by Moeller et al. (2012) in supplementary information (SI Table 2 and 3).

The external analytical reproducibility (standard deviation) calculated from replicate measurements of the certified stream sediments LGC6189 from United Kingdom Accreditation Service (including column duplicate, n=6) over multiple analytical sessions was 0.02‰ and $\delta^{66}Zn$ was determined at 0.18‰.

2.5 Data treatment

Metal (Pb, Zn, Cd, Tl, Hg) and metalloid (As, Sb) concentration in the sediment was normalized to Al concentration. Indeed, Al is a conservative element and a major constituent of the fine fraction (clay and fine silt) of sediments, which includes the particles most enriched in metals and metalloids (Owens et al., 2005). Al was used as a grain-size proxy and thus the normalization allowed taking into account the dilution effect by silica or calcite and compensating for the effect of grain size distribution (Bouchez et al., 2011). The Enrichment Factor (EF) was then calculated to assess the level of contamination relatively to a reference level:

$EF = (Me/Al)_{sample} / (Me/Al)_{reference}$

where $(Me/Al)_{sample}$ is the concentration ratio of a metal to Al in the sediment sample and $(Me/Al)_{reference}$ is the same ratio in the reference. To detect possible anthropogenic contamination, the reference should be representative of the local geochemical background (Meybeck, 2013). In this study, the selected reference was the average Me/Al ratio in the samples from the bottom of the sedimentary archive (layer GE1 to layer GE6) which represented the pre-industrial metal and metalloid content (Dezileau et al., 2013; Dezileau et al., in review). This approach allows to integrate the geological variability of the whole upstream watershed and to avoid local anomalies.

Concentrations ($\mu g.g^{-1}$) and enrichment factors (EF) are given for the sedimentary archive and the whole dataset of current stream sediments in supplementary information (SI Table 4 and 5).

Data analysis R software was used for all statistical analyses. Correlation factors (R^2) were calculated with Spearman method.

3 Results

3.1 Enrichment factors for the sedimentary archive and current stream sediments

In order to distinguish metals and metalloids of anthropogenic origin from natural sources, it is necessary to assess the local geochemical background, especially in a mining watershed where the concentrations in soils and sediments can be naturally high. The bottom of the sedimentary archive was considered as the geochemical background for the Gardon River watershed and used for further EF determination. This local geochemical background value was higher than the Upper Continental Crust average (Taylor and McLennan, 1995 for As, Sb, Cd, Pb, Zn and Tl; Wedepohl, 1995 for Hg) used in some studies as the reference level, by ~23-times for As, ~21-times for Sb, ~3-times for Cd, ~2.5-times for Pb, ~1.7-times for Zn and Tl and lower by ~2.3 times for Hg (Table 2).

3.1.1 Sedimentary archive

Enrichment factors (EF) of Pb, Zn, Cd, Tl, Hg, As and Sb in sediments of the archive are presented in Figure 2. For all these elements, EF values increased from the layer GE10 to upper layers, showing metal enrichment throughout time. For As and Pb, EF reached a plateau at 1.4 (As) and 1.8 (Pb) in the layers GE10 to GE17, and then increased substantially up to 1.9 (As) and 3.5 (Pb) in the layer GE18, assigned to 1969-dated flood event (Dezileau et al., 2013; Dezileau et al., in review). For Hg, EF value continuously increased from GE10 to GE17, the latter layer matching the 1963-dated flood event (Dezileau et al., 2013; Dezileau et al., in review), and then increased drastically in the layer GE18. For other elements (Zn, Cd, Tl and Sb), a general increase of EF value was observed from GE10 to GE18, reaching 2.1 for Zn, 3.5 for Cd, 1.9 for Tl, and 2.5 for Sb, although important variations were recorded from one layer to another and even within a single layer. For Sb, a peak was recorded in the layer GE7 whose deposition date was anterior to the beginning of large-scale mining activity on the catchment (Dezileau et al., 2013; Dezileau et al., in review).

The GE19 layer was particularly remarkable; a peak was recorded for all studied metals and metalloids and most markedly for As, Pb and Hg with EF value reaching respectively 9.9, 10.5 and 18. This layer was ascribed to an exceptional flood event in 1976 that caused important damage on tailings impoundment at the Pb/Zn Carnoulès mine (BRGM, BASOL

website). The most recent layer GE20, which corresponded to the latest exceptional flood event in 2002 (Delrieu et al., 2005), presented drastically lower EF values compared to those recorded in the 1976-dated layer; these values were similar to those recorded in 1969 for Pb, Zn, Cd, Tl and As. The order of metal and metalloid enrichment in the sedimentary archive was Hg>Cd>Sb>Pb>As>Zn≥Tl except for the layer GE19 for which As and Pb were more enriched than Cd, Sb, Tl and Zn.

3.1.2 Current stream sediments

EF values for current stream sediment sample collected at station 25, close to the location of the sedimentary archive are labeled in Figure 2, for comparison to historical record. For this sample, EF values were similar or slightly lower (for Cd) than the 2002 flood event layer values (Figures 2 and 3), thus reflecting comparable contamination level. In order to have an overview of spatial distribution of the contamination, EF values of sediments sampled in December 2012 (the most complete campaign) are mapped on the figure 4 using bar charts for sediments of the main stream and a dot with EF value for sediments of the tributaries. However, the whole dataset which is used for interpretation is presented in supplementary information (SI Table 5). Similar EF values were obtained at the station 25 and at the next upstream station 24, located downstream from the junction between the rivers Gardon of Ales and Gardon of Anduze (Figure 4). Upstream from this junction, at the station 11 in the Gardon of Ales River and station 23 in the Gardon of Anduze River, EF values were drastically higher for Hg (EF=6.6) and Sb (EF=5.7) and to a lesser extent for Zn (EF=4.9) and Cd (EF=4.6) in the Gardon of Ales River than in the Gardon of Anduze River (EF≈1.5, 1.5, 1.9 and 2.3 respectively). For other studied elements (Pb, As, Tl), EF values were similar at both stations, with average values EF of 3.7±0.7 for Pb, 2.3±0.1 for As, 1.7±0.3 for Tl. This indicated a significantly higher enrichment of Sb, Hg, Zn and Cd on the Gardon of Ales subwatershed compared to the Gardon of Anduze subwatershed while Pb, As, and Tl were slightly enriched on both subwatersheds.

For Sb and Hg, EF values for the main stream of the Gardon of Ales River increased from background level up to 7 (Sb) and 11.6 (Hg) from upstream to downstream stations below the Sb mine-impacted tributaries (AF1 and AF2) and the coal extraction area of La Grand-Combe respectively and then decreased downflow. This reflected a contribution of these sites to Sb and Hg enrichment in the main stream sediments of the Gardon of Ales River. Conversely, EF values for Sb and Hg in the main stream sediments of the Gardon of Anduze River was lower

than 2, which did not denote a significant contribution of the following Sb- and Hg-affected tributaries AF8 (EF = 57 for Sb, EF = 174 for Hg), AF9 (EF = 16 for Sb, EF = 35 for Hg) and AF10 (EF = 9.6 for Sb and EF = 24 for Hg). For other elements (Pb, Zn, As, Cd and Tl), a two-fold increase of EF values was observed for As, Zn, Cd, Tl and three-fold increase for Pb in the main stream sediments of the Gardon of Anduze downstream the tributaries AF8, AF9 and AF10 draining old Pb/Zn mines. Moreover, a two-fold increase was observed for As, Pb and Tl, a three-fold increase for Zn and five-fold increase for Cd in main stream sediments of the Gardon of Ales River downstream the town of Ales and the Grabieux River (AF4) which drained both Pb/Zn mines and urban area. An additional increase was also evidenced at downstream site (station 10) for Cd, reflecting the contribution of diffuse or unidentified point source.

3.2 Inter-element metal/aluminum ratio correlations

Inter-element Me/Al correlations may be used to characterize different groups of chemical elements with similar geochemical patterns. In the sedimentary archive, Me/Al values for Pb, Zn, Cd, Tl and As were highly correlated with each other ($0.71<R^2<0.87$) from GE1 to GE18 and in GE20 (Table 3); furthermore three groups of points representing (i) pre-industrial era (GE1 to GE9) (ii) industrial era until 1963 (GE10 to GE17) and (iii) industrial era in 1969 and 2002 (GE18 and GE20), were distributed along a dilution line in relation with the contamination level (Figure 3). This suggested a common origin for these elements over time. The correlation was slightly lower between these elements and Sb ($0.60<R^2<0.75$) or Hg ($0.56<R<0.77$). In the layer GE19 corresponding to the extreme 1976 flood event, the data did not follow the same dilution line as the other layers (Figure 3); showing a different geochemical signature.

In current main stream sediments, correlations were generally lower than in the sedimentary archive (Table 4). On the Gardon of Anduze River, positive correlations were observed between Pb, Zn, Cd, Tl, As and Hg ($0.23<R^2<0.93$). On the Gardon of Ales River, Pb, Zn, Cd, Tl and As were also correlated ($0.42<R^2<0.90$), while Hg was correlated only with As, Tl and Pb ($0.49<R^2<0.69$). Among these elements, Zn and Cd were highly correlated on both the Gardon of Anduze and the Gardon of Ales Rivers subwatersheds ($R^2=0.93$ and 0.91 respectively). No correlation was observed between Sb and the 6 other elements ($0.00<R^2<0.17$) on any of the subwatersheds indicating a different predominant source for Sb.

3.3 Zinc isotopes

Zinc isotopic composition was determined in the sedimentary archive (Figure 5a) and in current sediments from the Gardon River including some of its tributaries (Figure 5b). In the sedimentary archive, the range of variation of $\delta^{66}Zn$ was quite narrow, from 0.20 to 0.26‰ (Figure 5a). Extremely homogeneous values ($\delta^{66}Zn$=0.26 ± 0.02‰) were obtained in the bottom of the sedimentary archive, from GE1 to GE7, whereas significant variations occurred in upper layers.

Current stream sediments from the main stream of the Gardon River exhibited $\delta^{66}Zn$ values from 0.18 to 0.25‰, thus matching the range of the sedimentary archive (Figure 5b). The values tended to decrease from upstream to downstream sites along the main stream of the Gardon River. Zn-contaminated tributaries exhibited significantly lower ($\delta^{66}Zn$ = 0.07‰ for AF9 and 0.08‰ for AF10) or higher ($\delta^{66}Zn$ = 0.31‰ for AF6) $\delta^{66}Zn$ values.

3.4 Chemical partitioning of metals and metalloids

The chemical partitioning of Cd, Zn, Pb, Tl, As and Sb in the sedimentary archive is presented in Figure 6. The proportion of Cd, Zn, Pb, Tl and As contained in the most reactive fractions (F1+F2+F3) increased from the bottom to the top of the archive, following the increase of EF value. However, these metals and metalloids showed different distribution pattern. Cd was largely associated with the most reactive fractions (48%<F1+F2+F3<86%) and exhibited the highest proportion in exchangeable/carbonates fraction (F1), from 18±3% on average in the bottom layers (GE1 to GE9) up to 36.5% in the most contaminated layer (GE19). For Zn, the sum of the most reactive fractions (F1+F2+F3) increased gradually from 11±2% on average in the bottom layers (GE1 to GE9) to 49±5% on average in upper layers (GE19 to GE20), the distribution among fraction F1, F2 and F3 remaining homogeneous. The partitioning of Pb was dominated by Fe/Mn oxyhydroxides fraction (26%<F2<59%) with low exchangeable/carbonates and organic matter/sulfides fractions (F1<6% and F3<17%). Tl, As and Sb were mainly associated with the residual fraction (F4≥65.5%). For Tl and As, the Fe/Mn oxyhydroxides fraction (F2) represented up to 19% (Tl) and 25% (As).

Chemical partioning of Cd, Zn, Pb, Tl, As and Sb in current stream sediments from the Gardon River was similar to that of the sedimentary archive (Table 5). Cd and Zn exhibited the highest proportion in exchangeable/carbonates fraction F1, ranging from 25% to 62% for Cd and from 6% to 37% for Zn, with the most reactive fractions (F1+F2+F3) accounting

respectively for 71±12% and 40±16% (Table 5). For Pb, the reactive fractions represented 44±12% and were dominated by the Fe/Mn oxyhydroxides fraction (F2=30±8%). Tl and As were largely bound to the residual fraction (F4>56% and 75% respectively) with Fe/Mn oxyhydroxides fraction accounting for the majority of the remaining content. Sb was essentially contained in the residual fraction (F4>94%).

For Cd, Zn, Pb and to a lesser extent for Tl and As, the proportion of the most reactive fractions (F1+F2+F3) in main stream sediments tended to increase from upstream to downstream sites along the watershed in relation with increased EF value. F1+F2+F3 represented on average 62% for Cd, 27% for Zn, 40% for Pb, 6% for Tl and 12% for As in sediments of the upstream Gardon River (station 1, 3, 13 and 15) and reached 84% for Cd, 54% for Zn, 45% for Pb, 21% for Tl and 22% for As in sediments of downstream watershed at station 24 downstream from the junction between the Gardon of Anduze and the Gardon of Ales Rivers.

4 Discussion

4.1 Historical record of metal (Pb, Zn, Cd, Tl, Hg) and metalloid (As, Sb) contamination

The Gardon River watershed is a typical example of an ancient mining basin with multiple sources of metal contamination. The assessment of anthropogenic metal levels in this watershed and the deciphering of the origin of these contaminants is complex for several reasons: (1) the geology of the watershed, which includes several metal-mineralized areas, contributes to high metal levels in the transported sediments, thus confounding metals from anthropogenic origin, (2) the temporal variability of the hydrological regime, typical of the Mediterranean climate, with flash flood events responsible for most of the transport and deposition of polluted sediments in the riverbed and floodplain away from their contamination sources, making it difficult to acquire representative samples. Therefore, the use of a sedimentary archive, which integrates both anthropogenic metal emissions and geochemical background related to local geology of the whole upstream watershed, combined with current stream sediment analysis, can make sense for a rigorous estimation of the contamination status of the watershed. Sedimentary archives have recently been used to reconstruct watershed contamination histories in several European river basins (Audry et al., 2004b;

Ayrault et al., 2012; Ferrand et al., 2012; Gocht et al., 2001; Grosbois et al., 2012; Grousset et al., 1999; Le Cloarec et al., 2011; Monna et al., 2000; Müller et al., 2000; Winkels et al., 1998); these archives are generally floodplain cores (Ayrault et al., 2012; Gocht et al., 2001; Grosbois et al., 2012; Le Cloarec et al., 2011) or reservoir cores (Audry et al., 2004b; Müller et al., 2000). On the Gardon River watershed, there is no reservoir downstream from mining sites and it is very difficult to find intact continuous record in the floodplain mainly due to possible remobilization of sediments during flash floods which affect the watershed (Dezileau et al. in review; Delrieu et al. 2005). For these reasons, the sedimentary archive used was a high-standing flooding terrace which recorded only extreme flood events with a minimum discharge of 2100m^3/s (Dezileau et al., 2013; Dezileau et al., in review); the recording is thus discontinuous and provides a low temporal resolution. Nevertheless, the archive has recorded (i) pre-industrial floods allowing to determine the geochemical background of the watershed and (ii) 12 floods from the late 19th century to 2002 allowing to study the evolution of contamination level throughout the industrial era. Pre-industrial levels of Pb, Zn, Cd, Tl, Hg, As, and Sb in the archive allowed to characterize the local geochemical background of the Gardon River watershed, which was highly enriched for As, Sb and to a lesser extent for Cd, Pb, Zn and Tl relatively to the Upper Continental Crust, while being slightly depleted in Hg. These results point out the importance to assess the local reference level in mine-impacted watersheds for estimation of anthropogenic status as also highlighted elsewhere (Audry et al., 2004b; Dolgopolova et al., 2006; Lapworth et al., 2012). This high geochemical background for As, Sb, Cd, Pb, Zn and Tl in the Gardon watershed was related to the presence of several mineralized areas containing pyrite, galena, sphalerite and stibnite (BRGM, SIG Mines website; Alkaaby, 1986; European Comission 1988) on the Gardon of Ales and the Gardon of Anduze subwatersheds.

Since the late 19th century, 12 floods have been recorded by the sedimentary archive (layer GE9 to layer GE20), revealing a global enrichment of metals (Pb, Zn, Cd, Tl, Hg) and metalloids (As, Sb) in sediments of the Gardon River over time, until 1969, together with a contamination peak related to tailing dam failure in 1976 and a latest record in 2002 that presented levels similar to those of 1969 except for enrichment in Hg and Sb which was lower in 2002 than in 1969. This latest sedimentary record in 2002 might reflect remobilization of ancient floodplain sediments, acting as secondary contamination source during exceptional flooding events (Hudson-Edwards, 2003). However, the similarity of EF values in the 2002 sedimentary record and in current stream sediments (station 25), characterized by respectively

high (maximum discharge of 7200 m^3/s in 2002 (Dezileau et al., 2013; Dezileau et al., in review)) and moderate (1140 m^3/s in 2011, Banque Hydro website) intensity floods rather points out limited improvement of sediment quality over recent years. This historical pattern contrasted with that of large French Rivers such as the Loire River (Grosbois et al., 2012), the Seine River (Le Cloarec et al., 2011) or the Rhône River (Ferrand et al., 2012) where a gradual decrease was observed for most contaminants in sediments after 1980. This general decontamination has been explained by improvement of waste water treatment, de-industrialization and industrial processes changes and generally by more stringent environmental regulations (Ferrand et al., 2012; Grosbois et al., 2012; Le Cloarec et al., 2011; Meybeck, 2013).

4.2 Current sediment contamination

According to the classification of pollution level based on the enrichment factor method proposed by Sutherland (2000), current stream sediments were extremely polluted (EF>40), very highly polluted (20<EF<40) or significantly polluted (5<EF<20) for all studied elements (Pb, Zn, As, Cd, Tl, Sb and Hg) in sediments of mining/urban impacted tributary (AF4), mining/industrial impacted tributary (AF6) and Pb/Zn mines impacted tributaries (AF8, AF9 and AF10). Tributaries which drain old Sb mines (AF1 and AF2) were extremely polluted (AF1) and very highly polluted (AF2) with Sb.

In the sediments of the Gardon of Ales River, Hg and Sb were significantly (5<EF<20) to moderately (2<EF<5) enriched. In both the Gardon of Anduze and the Gardon of Ales Rivers, Pb, Zn, As and Cd were moderately enriched (2<EF<5) downstream from polluted tributaries (AF4, AF6, AF8, AF9, AF10) while EF values for Tl reflected no or minimal pollution signal in sediments. Variation of EF values along the Gardon of Ales and the Gardon of Anduze Rivers downstream from the uppermost affected tributaries differed for the following two groups of elements. For Pb, Zn, Cd, As and Tl, EF values remained almost constant, suggesting a continuous input of these elements by several polluted tributaries along the main stream (AF8, AF9 and AF10 on the Gardon of Anduze River and AF4, AF6 on the Gardon of Ales River). For Sb and Hg, the decrease of EF values along the flowpath may reflect the prevailing contribution of sources located on the upstream watershed and then the dilution by less contaminated sediments, hydraulic sorting or storage in reservoir and floodplain (Byrne et al., 2012; Hudson-Edwards, 2003).

4.3 Sources of metals and metalloids in the sedimentary archive and current stream sediments

Metal/aluminum ratios Pb, As, Zn, Cd and Tl in the sedimentary archive were found to be correlated, suggesting a common origin for these elements from the pre-industrial era until the present day. Such correlation could be ascribed to the association of these elements within the Pb/Zn mineralization that has been exploited in several mines on the Gardon of Ales and the Gardon of Anduze subwatersheds. This mineralization contained traces of cadmium in sphalerite (ZnS), arsenic in Fe-sulfides (pyrite, marcasite FeS_2), in sulfosalts (proustite Ag_3AsS_3) and in galena (PbS), antimony in sulfosalts (pyrargyrite Ag_3SbS_3) and in galena, mercury in Fe-sulfides and in sphalerite and thallium in Fe-sulfides (Alkaaby, 1986; Casiot et al., 2011; European Comission, 1988). In particular, the strong relationship between Zn and Cd both in the archive and in current stream sediments might reflect a homogeneous Cd content in Zn-ore in the area. The 1976 layer exhibited a different geochemical signature, with enrichment of As and Pb compared to previous layers; this was a local characteristic of flotation residues stored behind a dam at the abandoned Carnoulès site located 60 km upstream from the archive location (Leblanc et al., 1996); the impoundment contained As-rich pyrite and galena, the wastes having exceptionally high As (~0.2%) and Pb (~0.7%) content. Correlations of metal/aluminum ratios for Sb and Hg with other studied metal or metalloid were lower than for the other elements, suggesting a contribution of multiple sources including the Pb/Zn mineralization (Alkaaby, 1986) and Pb/Zn mine-impacted tributaries (AF4, AF6, AF8, AF9 and AF10). However, the spatial distribution of EF values for Sb in current stream sediments suggested that extraction of Sb ore and smelting works on the upstream subwatershed of the Gardon of Ales River were responsible for the Sb enrichment in main stream sediments of the Gardon River. The contamination peak at the bottom of the sedimentary archive probably reflected ancient mining works dating back to the early 19th century; first extraction (1810-1858) and smelting activities (1833-1858) were operating near the tributary AF2. Then the largest Sb mine was active between 1906 and 1948 resulting in 38,000T of tailings drained by the tributary AF1 and an associated smelter that worked between 1896 and 1951 (BRGM, BASIAS website). For Hg, important enrichment evidenced in current main stream sediments of the Gardon of Ales River downstream from the coal production area of La Grand-Combe suggests the predominance of this source over Pb-Zn mineralization.

The potential of Zn isotopes to track the sources of zinc have been investigated in the present study because Zn enrichment in current main stream sediments was evidenced downstream various sources (Pb/Zn mine-impacted tributaries AF8, AF9 and AF10; both urban and mine-impacted tributary AF4, both industrial and mine-impacted tributary AF6; Ales town). However, considering the prevailing Pb/Zn mining origin for Zn in sediments of the Gardon River watershed, the relatively uniform isotopic composition of the sedimentary archive and current main stream sediments (δ^{66}Zn=0.23±0.03‰) was consistent. Nevertheless, significant differences were evidenced between the relatively homogeneous values at the bottom of the sedimentary archive and upper layers, also between current main stream sediments and tributaries. δ^{66}Zn value of the natural geochemical background of the Gardon River watershed was 0.26‰±0.02‰, lying within background values determined at 0.31±0.06‰ for the Lot River watershed (Sivry et al., 2008), also located in the Massif Central Mountains in France. Local Zn-ore was found at 0.18‰ (unpublished data) which is close to the δ^{66}Zn average of 0.16‰ proposed by Sonke et al. (2008) for sphalerite. δ^{66}Zn values in upper layers (from GE8 to GE20) of the sedimentary archive and in current main stream sediments impacted by anthropogenic activities deviated slightly from the background value, with an average of 0.20‰ in the sedimentary archive and 0.18‰ in current main stream sediments. This was consistent with the contribution of Pb/Zn mine-impacted tributaries (AF9, AF10), characterized by lower δ^{66}Zn value (~0.07‰), to Zn enrichment in main stream sediments.

Conversely, the higher δ^{66}Zn value of tributary AF4 (δ^{66}Zn = 0.31‰), both influenced by industrial and mining sites, did not significantly increase the δ^{66}Zn value of the main stream, showing little impact of industrial Zn source on Zn load. δ^{66}Zn values of polluted sediments from this study were drastically lower than in reservoir sediments of the Lot River downstream from the mining and smelting area of Decazeville (δ^{66}Zn=0.75 to 1.35‰), where the smelting process favored enrichment in the heavier isotopes in the remaining waste (Sivry et al., 2008). In the present study, ancient smelting activities on the Gardon of Ales subwatershed, at La Grand-Combe (Ministère de la Culture) did not appear to significantly influence δ^{66}Zn value in the sediments from this watershed.

To our knowledge, the δ^{66}Zn data presented in this study are the first for riverbed sediments from AMD-impacted streams. They showed an isotopic composition at δ^{66}Zn~0.07‰, thus within the range of 0.02 to 0.46‰ measured for the water compartment in a variety of streams draining historical mining district in United States and Europe (Borrok et al., 2008). This

lower value for AMD-impacted sediments compared to the local Zn-ore ($\delta^{66}Zn$=0.18‰) was unexpected considering the low isotopic fractionation during Zn sulfide dissolution (Fernandez and Borrok, 2009) and the preferential uptake of heavier Zn isotopes during adsorption on ferrihydrite, which precipitates in AMD-impacted rivers (Aranda et al., 2012; Balistrieri et al., 2008; Borrok et al., 2008). However, it probably reflects the complex processes leading to enrichment either in the heavier or in the lighter isotopes depending on the mineral phase onto which Zn is sorbed (Pokrovsky et al., 2005). Moreover, Borrok et al. (2008) highlighted that lighter isotopes are enriched in the solid reservoir during important diel fluctuations of dissolved Zn concentrations. Considering the variety of processes involved in the cycle of Zn in AMD-impacted streams, further research would be required to elucidate those controlling Zn isotopic composition in our mine-impacted streambed sediments.

4.4 Environmental significance of metal partitioning in sediments

Considering the relatively high enrichment factors for the studied metals and metalloids in the sediments of the Gardon River watershed, it is important to evaluate the potential mobility of these elements in the sediments that can act as a chemical sink or a potential source of pollutants to the overlying water. The three first fractions (F1, F2 and F3) define as exchangeable, reducible and oxidisable fractions are supposed to contain metals that may be mobilized toward the aqueous phase by changing redox conditions i.e. from reducing to oxidizing (floods, dredging), and conversely from oxidizing to reducing (early diagenesis) or pH conditions (Byrne et al., 2012). Subsequently to their release, metals may be transported downstream in the dissolved phase or they might re-distribute to another solid phase in the sediment (Audry et al., 2010; Byrne et al., 2012). Considering the percentage of metals and metalloids extracted in the fractions F1+F2+F3, the order of potential mobility in the sedimentary archive and in current stream sediments was Sb (1-7%) < Tl (3-34%) = As (4-35%) < Zn (9-65%) < Pb (25-77%) < Cd (48-88%). Comparison with other studies is limited due to the diversity of the extraction protocols used (Byrne et al., 2012; Filgueiras et al., 2002). Nevertheless, other authors using BCR procedure or a similar one also reported an important potential mobility for Cd, Zn and Pb in mine affected rivers. For As and Sb, geochemical associations and subsequent estimation of their potential mobility in mine-affected stream sediments differed widely through studies. Galán et al. (2003) showed that As was mainly bound to the relatively mobile pool in poorly cristallized Fe and Mn

oxyhydroxides (fraction F2) in acidic Odiel and Tinto Rivers (Spain) affected by AMD while other studies reported low mobility for As in other mining impacted environments (Bird et al., 2003; Grosbois et al., 2001; Rapant et al., 2006). Association of Sb to the residual fraction evidenced in other mine-impacted watersheds (Grosbois et al., 2001; Kraus and Wiegand, 2006; Rapant et al., 2006) was ascribed to its presence in stibnite which is an insoluble sulfide phase (Kraus and Wiegand, 2006).

An increase of the proportion of the most reactive fractions (F1+F2+F3) was observed in relation with EF increase for Cd, Zn, Pb and to a lesser extent for As and Tl both in the sedimentary archive and in current main stream sediments of the Gardon River. Such an increase of metal mobility associated to anthropogenic contamination was already observed in other mining environments (Byrne et al., 2012) and industrial or urban affected rivers (Gagnon et al., 2009; Kim et al., 2009) showing that sediments may not act as a permanent sink for these metals.

5 Conclusion

This study provided evidence of the gradual enrichment of Pb, Zn, Cd, Tl, Hg, As and Sb in the sediments of the Gardon watershed since the late 19th century related to the beginning of the industrial era and a remaining contamination pattern in recent decades, in contrast to the general decontamination observed for large French Rivers.

The combination of inter-element relationships and spatial distribution of EF values allowed to point out the main sources of metals and metalloids in sediments, i.e. Pb/Zn ore exploitation (Pb, Zn, As, Tl, Cd), antimony mining (Sb) and coal extraction (Hg). Zinc isotopic composition provided modestly useful complement to the traditional geochemistry results, in this particular context. The contribution of lighter $\delta^{66}Zn$ value of AMD-impacted streams decreases only slightly the isotopic composition of the Gardon River sediments. Anthropogenic enrichment of metals and metalloids from mining origin in sediments of the Gardon River was associated to increased potential mobility, as estimated by sequential extraction, for Cd, Pb, Zn and to a lesser extent for As and Tl.

Altogether, these results showed that about fifty years after the closure of mines, the former mining sites remained the prevailing sources of Pb, Zn, Cd, Tl, Hg, As and Sb in sediments of the Gardon River, some of these contaminants initially trapped in the sediment being

potentially mobilizable toward the aqueous medium by changing environmental conditions. Further studies are necessary to quantify the contribution of specific mining sites to global metal and metalloid enrichment in sediments of the Gardon River and to determine if these sediments may actually become a source of contaminant to the overlying water.

6 Acknowlegments

The authors would like to thank Sophie Delpoux for fieldwork and analysis and Daniel Cossa for mercury analysis. Jérôme Chmeleff and Philippe Télouk are gratefully acknowledged for zinc isotopic analysis at Toulouse and Lyon. This study was supported by the EC2CO-INSU program and OSU OREME (http://www.oreme.univ-montp2.fr).

References

Alkaaby, A. (1986). Conglomérats minéralisés (Pb-Ba-Fe) du Trias basal sur la bordure sud-est des Cévennes : exemple du système fluvial en tresse de Carnoulès (Gard). Thesis. Université des Sciences et Techniques du Languedoc. p.154.

Aranda, S., Borrok, D. M., Wanty, R. B., & Balistrieri, L. S. (2012). Zinc isotope investigation of surface and pore waters in a mountain watershed impacted by acid rock drainage. The Science of the Total Environment, 420, 202–213.

Audry, S., Schäfer, J., Blanc, G., Bossy, C., & Lavaux, G. (2004a). Anthropogenic components of heavy metal (Cd, Zn, Cu, Pb) budgets in the Lot-Garonne fluvial system (France). Applied Geochemistry, 19(5), 769–786. doi:10.1016/j.apgeochem.2003.10.002

Audry, S., Schäfer, J., Blanc, G., & Jouanneau, J.-M. (2004b). Fifty-year sedimentary record of heavy metal pollution (Cd, Zn, Cu, Pb) in the Lot River reservoirs (France). Environmental Pollution, 132(3), 413–426. doi:10.1016/j.envpol.2004.05.025

Audry, S., Grosbois, C., Bril, H., Schäfer, J., Kierczak, J., & Blanc, G. (2010). Post-depositional redistribution of trace metals in reservoir sediments of a mining/smelting-impacted watershed (the Lot River, SW France). Applied Geochemistry, 25(6), 778–794. doi:10.1016/j.apgeochem.2010.02.009

Ayrault, S., Roy-Barman, M., Le Cloarec, M.-F., Priadi, C. R., Bonté, P., & Göpel, C. (2012). Lead contamination of the Seine River, France: geochemical implications of a historical perspective. Chemosphere, 87(8), 902–910. doi:10.1016/j.chemosphere.2012.01.043

Balistrieri, L. S., Borrok, D. M., Wanty, R. B., & Ridley, W. I. (2008). Fractionation of Cu and Zn isotopes during adsorption onto amorphous Fe(III) oxyhydroxide: Experimental mixing of acid rock drainage and ambient river water. Geochimica et Cosmochimica Acta, 72(2), 311–328.

Banque Hydro, Eaufrance. Last accessed on 11/26/2013. http://www.hydro.eaufrance.fr/

Bird, G., Brewer, P. A., Macklin, M. G., Balteanu, D., Driga, B., Serban, M., & Zaharia, S. (2003). The solid state partitioning of contaminant metals and As in river channel sediments of the mining affected Tisa drainage basin, northwestern Romania and eastern Hungary. Applied Geochemistry, 18(10), 1583–1595. doi:10.1016/S0883-2927(03)00078-7

Bonilla-Valverde, D., Ruiz-Laguna, J., Muñoz, A., Ballesteros, J., Lorenzo, F., Gómez-Ariza, J. L., & López-Barea, J. (2004). Evolution of biological effects of Aznalcóllar mining spill in the Algerian mouse (Mus spretus) using biochemical biomarkers. Toxicology, 197(2), 123–138. doi:10.1016/j.tox.2003.12.010

Borrok, D. M., Nimick, D. A., Wanty, R. B., & Ridley, W. I. (2008). Isotopic variations of dissolved copper and zinc in stream waters affected by historical mining. Geochimica et Cosmochimica Acta, 72(2), 329–344. doi:10.1016/j.gca.2007.11.014

Borrok, D. M., Wanty, R. B., Ridley, W. I., Lamothe, P. J., Kimball, B. A., Verplanck, P. L., & Runkel, R. L. (2009). Application of iron and zinc isotopes to track the sources and mechanisms of metal loading in a mountain watershed. Applied Geochemistry, 24(7), 1270–1277. doi:10.1016/j.apgeochem.2009.03.010

Bouchez, J., Lupker, M., Gaillardet, J., France-Lanord, C., & Maurice, L. (2011). How important is it to integrate riverine suspended sediment chemical composition with depth? Clues from Amazon River depth-profiles. Geochimica et Cosmochimica Acta, 75(22), 6955–6970.

BRGM, SIG Mines. Last accessed on 11/26/2013. http://sigminesfrancebrgmfr/

BRGM, InfoTerre. Last accessed on 11/26/2013. http://infoterre.brgm.fr/

BRGM, BASIAS. Inventaire historique de sites industriels et activités de service. Last accessed on 11/26/2013. http://basias.brgm.fr/

BRGM, BASOL. Last accessed on 11/26/2013. http://basol.developpement-durable.gouv.fr/

Byrne, P., Wood, P. J., & Reid, I. (2012). The Impairment of River Systems by Metal Mine Contamination: A Review Including Remediation Options. Critical Reviews in Environmental Science and Technology, 42(19), 2017–2077. doi:10.1080/10643389.2011.574103

Caruso, B., Cox, T., Runkel, R., Velleux, M., Bencala, K., Nordstrom, D., Julien, PY., Butler, BA., Alpers, CN.,Marion, A., & Smith, K. (2008). Metals fate and transport modelling in streams and watersheds: state of the science and USEPA workshop review. Hydrological Processes, 22, 4011–4021. doi:10.1002/hyp

Casiot, C., Egal, M., Bruneel, O., Verma, N., Parmentier, M., & Elbaz-Poulichet, F. (2011). Predominance of aqueous Tl (I) species in the river system downstream from the abandoned Carnoules Mine (Southern France). Environmental Science & Technology, 45(I), 2056–2064.

Casiot, C., Egal, M., Elbaz-Poulichet, F., Bruneel, O., Bancon-Montigny, C., Cordier, M.-A., Gomez, E., & Aliaume, C. (2009). Hydrological and geochemical control of metals and arsenic in a Mediterranean river contaminated by acid mine drainage (the Amous River, France); preliminary assessment of impacts on fish (Leuciscus cephalus). Applied Geochemistry, 24(5), 787–799. doi:10.1016/j.apgeochem.2009.01.006

Chen, J., Gaillardet, J., & Louvat, P. (2008). Zinc Isotopes in the Seine River Waters, France: A Probe of Anthropogenic Contamination. Environmental Science & Technology, 42(17), 6494–6501. doi:10.1021/es800725z

Chen, J., Gaillardet, J., Louvat, P., & Huon, S. (2009). Zn isotopes in the suspended load of the Seine River, France: Isotopic variations and source determination. Geochimica et Cosmochimica Acta, 73(14), 4060–4076. doi:10.1016/j.gca.2009.04.017

Cloquet, C., Carignan, J., & Libourel, G. (2006). Isotopic composition of Zn and Pb atmospheric depositions in an urban/Periurban area of northeastern France. Environmental Science & Technology, 40(21), 6594–600.

Cloquet, C., Carignan, J., Lehmann, M. F., & Vanhaecke, F. (2008). Variation in the isotopic composition of zinc in the natural environment and the use of zinc isotopes in biogeosciences: a review. Analytical and bioanalytical chemistry, 390(2), 451–63. doi:10.1007/s00216-007-1635-y

Cherry, D. S., Currie, R. J., Soucek, D. J., Latimer, H. A., & Trent, G. C. (2001). An integrative assessment of a watershed impacted by abandoned mined land discharges. Environmental Pollution, 111(3), 377–88.

Delrieu, G., Ducrocq, V., Gaume, E., Nicol, J., Payrastre, O., Yates, E., Kirstetter, PE., Andrieu, H., Ayral, PA., Bouvier, C., Creutin, JD., Livet, M., Anquetin, S., Lang, M., Neppel, L., Obled, C., Parent-Du-Chatelet, J., Saulier, GM., Walpersdorf, A., & Wobrock, W. (2005). The catastrophic flash-flood event of 8-9 September 2002 in the Gard region, France: a first case study for the Cévennes-Vivarais Mediterranean Hydrometeorological. Journal of Hydrometeorology, 6, 34–52.

Dezileau, L., Terrier, B., Berger, J. F., Blanchemanche, P., Freydier, R., Bremond, L., Latapie, A., Paquier, A., Lang, M., & Delgado, J. (in review). A multi-dating approach applied to historical slackwater flood deposits of the Gardon River, SE France. Geomorphology.

Dezileau, L., Terrier, B., Berger, J. F., Blanchemanche, P., Freydier, R., Latapie, A., Paquier, A., Lang, M., & Delgado, J. (2013). Reconstitution des crues extrêmes du Gardon à partir d'une analyse paléohydrologique. In Société Hydrotechnique de France (pp. 1–12).

Dolgopolova, A., Weiss, D. J., Seltmann, R., Kober, B., Mason, T. F. D., Coles, B., & Stanley, C. J. (2006). Use of isotope ratios to assess sources of Pb and Zn dispersed in the environment during mining and ore processing within the Orlovka–Spokoinoe mining site (Russia). Applied Geochemistry, 21(4), 563–579. doi:10.1016/j.apgeochem.2005.12.014

Ettler, V., Mihaljevic, M., Sebek, O., Molek, M., Grygar, T., & Zeman, J. (2006). Geochemical and Pb isotopic evidence for sources and dispersal of metal contamination in stream sediments from the mining and smelting district of Príbram, Czech Republic. Environmental Pollution, 142(3), 409–417. doi:10.1016/j.envpol.2005.10.024

European Comission. (1988). Summary reports of the subprogramme: metals and mineral substances (1982-85): Volume 1. (M. Donato & L. Van Wambeke, Eds.) (Commission., Vol. 1, p. 552).

Fernandez, A., & Borrok, D. M. (2009). Fractionation of Cu, Fe, and Zn isotopes during the oxidative weathering of sulfide-rich rocks. Chemical Geology, 264, 1–12. doi:10.1016/j.chemgeo.2009.01.024

Ferrand, E., Eyrolle, F., Radakovitch, O., Provansal, M., Dufour, S., Vella, C., Raccasi, G., & Gurriaran, R. (2012). Historical levels of heavy metals and artificial radionuclides

reconstructed from overbank sediment records in lower Rhône River (South-East France). Geochimica et Cosmochimica Acta, 82, 163–182. doi:10.1016/j.gca.2011.11.023

Filgueiras, A. V., Lavilla, I., & Bendicho, C. (2002). Chemical sequential extraction for metal partitioning in environmental solid samples. Journal of Environmental Monitoring, 4(6), 823–857. doi:10.1039/b207574c

Gagnon, C., Turcotte, P., & Vigneault, B. (2009). Comparative study of the fate and mobility of metals discharged in mining and urban effluents using sequential extractions on suspended solids. Environmental Geochemistry and Health, 31(6), 657–671. doi:10.1007/s10653-008-9223-4

Galán, E., Gómez-Ariza, J., Gonzales, I., Fernandez-Caliani, J., Morales, E., & Giraldez, I. (2003). Heavy metal partitioning in river sediments severely polluted by acid mine drainage in the Iberian Pyrite Belt. Applied Geochemistry, 18, 409–421.

Gocht, T., Moldenhauer, K., & Püttmann, W. (2001). Historical record of polycyclic aromatic hydrocarbons (PAH) and heavy metals in floodplain sediments from the Rhine River (Hessisches Ried, Germany). Applied Geochemistry, 16, 1707–1721.

Gosar, M., & Miler, M. (2011). Anthropogenic metal loads and their sources in stream sediments of the Meža River catchment area (NE Slovenia). Applied Geochemistry, 26(11), 1855–1866. doi:10.1016/j.apgeochem.2011.06.009

Gray, N. (1997). Environmental impact and remediation of acid mine drainage: a management problem. Environmental Geology, 30, 62–71.

Grimalt, J. O., Ferrer, M., & Macpherson, E. (1999). The mine tailing accident in Aznalcollar. The Science of the Total Environment, 242, 3–11.

Grosbois, C, Meybeck, M., Lestel, L., Lefèvre, I., & Moatar, F. (2012). Severe and contrasted polymetallic contamination patterns (1900-2009) in the Loire River sediments (France). The Science of the Total Environment, 435-436, 290–305. doi:10.1016/j.scitotenv.2012.06.056

Grosbois, Cecile, Horowitz, A. J., Smith, J. J., & Elrick, K. A. (2001). The effect of mining and related activities on the sediment-trace element geochemistry of Lake Coeur d'Alene, Idaho, USA. Part III. Downstream effects: the Spokane River Basin. Hydrological Processes, 15(5), 855–875.

Grousset, F. E., Jouanneau, J. M., Castaing, P., Lavaux, G., & Latouche, C. (1999). A 70 year Record of Contamination from Industrial Activity Along the Garonne River and its Tributaries (SW France). Estuarine, Coastal and Shelf Science, 48(3), 401–414. doi:10.1006/ecss.1998.0435

Hudson-Edwards, K. (2003). Sources, mineralogy, chemistry and fate of heavy metal-bearing particles in mining-affected river systems. Mineralogical Magazine, 67(2), 205–217. doi:10.1180/0026461036720095

Hudson-Edwards, K., Macklin, M., & Taylor, M. (1997). Historic metal mining inputs to Tees river sediment. The Science of the Total Environment, 194/195, 437–445.

Jarvis, A., & Younger, P. (1997). Dominating chemical factors in mine water induced impoverishment of the invertebrate fauna of two streams in the Durham Coalfield, UK. Chemistry and Ecology, 13(4), 249–270.

Johnson, D. B., & Hallberg, K. B. (2005). Acid mine drainage remediation options: a review. The Science of the Total Environment, 338, 3–14. doi:10.1016/j.scitotenv.2004.09.002

Kim, Y., Kim, B.-K., & Kim, K. (2009). Distribution and speciation of heavy metals and their sources in Kumho River sediment, Korea. Environmental Earth Sciences, 60(5), 943–952. doi:10.1007/s12665-009-0230-2

Kimball, B. A., & Runkel, R. L. (2009). Spatially Detailed Quantification of Metal Loading for Decision Making: Metal Mass Loading to American Fork and Mary Ellen Gulch, Utah. Mine Water and the Environment, 28(4), 274–290. doi:10.1007/s10230-009-0085-5

Kraus, U., & Wiegand, J. (2006). Long-term effects of the Aznalcóllar mine spill-heavy metal content and mobility in soils and sediments of the Guadiamar river valley (SW Spain). The Science of the Total Environment, 367, 855–71. doi:10.1016/j.scitotenv.2005.12.027

Lapworth, D., Knights, K., Key, R., Johnson, C., Ayoade, E., Adekanmi, M., Arisekola, T., Okunlola, O., Backman, B., Eklund, M., Everett, P., Lister, R., Ridgway, J., Watts, M., Kemp, SJ., & Pitfield, P. (2012). Geochemical mapping using stream sediments in west-central Nigeria: Implications for environmental studies and mineral exploration in West Africa. Applied Geochemistry, 27(6), 1035–1052. doi:10.1016/j.apgeochem.2012.02.023

Le Cloarec, M.-F., Bonte, P. H., Lestel, L., Lefèvre, I., & Ayrault, S. (2011). Sedimentary record of metal contamination in the Seine River during the last century. Physics and Chemistry of the Earth, Parts A/B/C, 36(12), 515–529. doi:10.1016/j.pce.2009.02.003

Leblanc, M., Achard, B., Othman, D. Ben, & Luck, J. (1996). Accumulation of arsenic from acidic mine waters by ferruginous bacterial accretions (stromatolites). Applied Geochemistry, 11(96), 541–554.

MacKenzie, A., & Pulford, I. (2002). Investigation of contaminant metal dispersal from a disused mine site at Tyndrum, Scotland, using concentration gradients and stable Pb isotope ratios. Applied Geochemistry, 17(8), 1093–1103. doi:10.1016/S0883-2927(02)00007-0

Macklin, M., Brewer, P., & Balteanu, D. (2003). The long term fate and environmental significance of contaminant metals released by the January and March 2000 mining tailings dam failures in Maramureş County, upper Tisa Basin, Romania. Applied Geochemistry, 18, 241–257.

Macklin, M. G., Brewer, P. A., Hudson-Edwards, K. A., Bird, G., Coulthard, T. J., Dennis, I. A., Lechler, P.J., Miller, J.R., & Turner, J. N. (2006). A geomorphological approach to

the management of rivers contaminated by metal mining. Geomorphology, 79, 423–447. doi:10.1016/j.geomorph.2006.06.024

Macklin, M. G., Hudson-Edwards, K. A., & Dawson, E. J. (1997). The significance of pollution from historic metal mining in the Pennine orefields on river sediment contaminant fluxes to the North Sea. The Science of The Total Environment, 194-195(96), 391–397. doi:10.1016/S0048-9697(96)05378-8

Maréchal, C., Télouk, P., & Albarède, F. (1999). Precise analysis of copper and zinc isotopic compositions by plasma-source mass spectrometry. Chemical Geology, 156, 251–273.

Mattielli, N., Petit, J. C. J., Deboudt, K., Flament, P., Perdrix, E., Taillez, A., Rimetz-Planchon J. & Weiss, D. (2009). Zn isotope study of atmospheric emissions and dry depositions within a 5 km radius of a Pb–Zn refinery. Atmospheric Environment, 43(6), 1265–1272. doi:10.1016/j.atmosenv.2008.11.030

Mayes, W. M., Johnston, D., Potter, H. A. B., & Jarvis, A. P. (2009). A national strategy for identification, prioritisation and management of pollution from abandoned non-coal mine sites in England and Wales. I. Methodology development and initial results. The Science of the Total Environment, 407(21), 5435–47. doi:10.1016/j.scitotenv.2009.06.019

Meybeck, M. (2013). Heavy metal contamination in rivers across the globe : an indicator of complex interactions between societies and catchments. In Proceedings f H04 Understanding Freshwater Quality Problems in a Changing World (Vol. 361, pp. 3–16).

Michard, G., & Faucherre, J. (1970). Étude géochimique de l'altération des minerais sulfurés de St. Sébastien d'Aigrefeuille. Chemical Geology, 6, 63–84.

Mighanetara, K., Braungardt, C. B., Rieuwerts, J. S., & Azizi, F. (2009). Contaminant fluxes from point and diffuse sources from abandoned mines in the River Tamar catchment, UK. Journal of Geochemical Exploration, 100, 116–124. doi:10.1016/j.gexplo.2008.03.003

Miller, J. (1997). The role of fluvial geomorphic processes in the dispersal of heavy metals from mine sites. Journal of Geochemical Exploration, 58, 101–118.

Ministère de la Culture, Inventaire général du patrimoine culturel, base de donnée Mérimée. Last accessed on 11/26/2013. http://www.inventaire.culture.gouv.fr/

Moeller, K., Schoenberg, R., Pedersen, R.-B., Weiss, D., & Dong, S. (2012). Calibration of the New Certified Reference Materials ERM-AE633 and ERM-AE647 for Copper and IRMM-3702 for Zinc Isotope Amount Ratio Determinations. Geostandards and Geoanalytical Research, 36(2), 177–199. doi:10.1111/j.1751-908X.2011.00153.x

Monna, F., Camizuli, E., Revelli, P., Biville, C., Thomas, C., Losno, R., Scheifler, R., Bruguier, O., Baron, S., Chateau, C., Ploquin, A., & Alibert, P. (2011). Wild brown trout affected by historical mining in the Cévennes National Park, France. Environmental science & technology, 45(16), 6823–30. doi:10.1021/es200755n

Monna, F., Hamer, K., Lévêque, J., & Sauer, M. (2000). Pb isotopes as a reliable marker of early mining and smelting in the Northern Harz province (Lower Saxony, Germany). Journal of Geochemical Exploration, 68, 201–210.

Moore, J., & Luoma, S. (1990). Hazardous wastes from large-scale metal extraction. A case study. Environmental Science & Technology, 24(9), 1278–1285.

Moore, J. N., & Langner, H. W. (2012). Can a river heal itself? Natural attenuation of metal contamination in river sediment. Environmental Science & Technology, 46(5), 2616–2623. doi:10.1021/es203810j

Müller, J., Ruppert, H., Muramatsu, Y., & Schneider, J. (2000). Reservoir sediments–a witness of mining and industrial development (Malter Reservoir, eastern Erzgebirge, Germany). Environmental Geology, 39(12), 1341–1351.

Nriagu, J., & Pacyna, J. (1988). Quantitative assessment of worldwide contamination of air, water and soils by trace metals. Nature, 333, 134–139.

Owens, P. N., Batalla, R. J., Collins, A. J., Gomez, B., Hicks, D. M., Horowitz, A. J., Kondolf, G., Marden, M., Page, M., Peacock, D., Petticrew, E., Salomons, W., & Trustrum, N. (2005). Fine-grained sediment in river systems: environmental significance and management issues. River Research and Applications, 21(7), 693–717. doi:10.1002/rra.878

Peplow, D., & Edmonds, R. (2005). The effects of mine waste contamination at multiple levels of biological organization. Ecological Engineering, 24, 101–119. doi:10.1016/j.ecoleng.2004.12.011

Pokrovsky, O. S., Viers, J., & Freydier, R. (2005). Zinc stable isotope fractionation during its adsorption on oxides and hydroxides. Journal of colloid and interface science, 291(1), 192–200. doi:10.1016/j.jcis.2005.04.079

Rapant, S., Dietzová, Z., & Cicmanová, S. (2006). Environmental and health risk assessment in abandoned mining area, Zlata Idka, Slovakia. Environmental Geology, 51(3), 387–397. doi:10.1007/s00254-006-0334-x

Rauret, G., López-Sánchez, J. F., Sahuquillo, A., Rubio, R., Davidson, C., Ure, A., & Quevauviller, P. (1999). Improvement of the BCR three step sequential extraction procedure prior to the certification of new sediment and soil reference materials. Journal of Environmental Monitoring, 1(1), 57–61.

Rolley, J., La petite histoire du plomb et du zinc en Cévennes. Last accessed on 11/26/2013. http://www.rolley.fr/Geologie.html

Rosman, K.J.R., & Taylor, P.D.P. (1998). Isotopic compositions of the elements 1997 (Technical Report). Pure and Applied Chemistry, 70(1), 217–235.

Salomons, W. (1995). Environmental impact of metals derived from mining activities: processes, predictions, prevention. Journal of Geochemical Exploration, 52, 5–23.

Schwarzenbach, R. P., Egli, T., Hofstetter, T. B., von Gunten, U., & Wehrli, B. (2010). Global Water Pollution and Human Health. Annual Review of Environment and Resources, 35(1), 109–136. doi:10.1146/annurev-environ-100809-125342

Sivry, Y., Riotte, J., Sonke, J., Audry, S., Schafer, J., Viers, J., Blanc, G., Freydier, R., & Dupre, B. (2008). Zn isotopes as tracers of anthropogenic pollution from Zn-ore smelters The Riou Mort–Lot River system. Chemical Geology, 255, 295–304. doi:10.1016/j.chemgeo.2008.06.038

SMAGE des Gardons (2011). Etude de la qualité des eaux du bassin des Gardons (p. 380).

Sonke, J., Sivry, Y., Viers, J., Freydier, R., Dejonghe, L., Andre, L., Aggarwal, J., Fontan, F., & Dupre, B. (2008). Historical variations in the isotopic composition of atmospheric zinc deposition from a zinc smelter. Chemical Geology, 252, 145–157. doi:10.1016/j.chemgeo.2008.02.006

Sutherland, R. (2000). Bed sediment-associated trace metals in an urban stream, Oahu, Hawaii. Environmental Geology, 39(6), 611–627.

Taylor, S. R., & McLennan, S. M. (1995). The geochemical evolution of the continental crust. Reviews of Geophysics, 33(2), 241–265.

Thapalia, A., Borrok, D., Van Metre, P., Musgrove, M., & Landa, E. (2010). Zn and Cu isotopes as tracers of anthropogenic contamination in a sediment core from an urban lake. Environmental Science & Technology, 44(5), 1544–50. doi:10.1021/es902933y

Vincent, M. (2006). Les Mines des Cevennes. (Terre Cevenole, Ed.) (p. 320).

Wedepohl, K. H. (1995). The composition of the continental crust. Geochimica et Cosmochimica Acta, 59(7), 1217–1232.

Weiss, D., Rehkdmper, M., Schoenberg, R., McLaughlin, M., Kirby, J., Campbell, P., Arnold T., Chapman J., Peel K. & Gioia, S. (2008). Application of nontraditional stable-isotope systems to the study of sources and fate of metals in the environment. Environmental Science & Technology, 42(3), 655–664.

Winkels, H. J., Kroonenberg, S. B., Lychagin, M. Y., Marin, G., Rusakov, G. V., & Kasimov, N. S. (1998). Geochronology of priority pollutants in sedimentation zones of the Volga and Danube delta in comparison with the Rhine delta. Applied Geochemistry, 13(5), 581–591. doi:10.1016/S0883-2927(98)00002-X

Younger, P., & Wolkersdorfer, C. (2004). Mining impacts on the fresh water environment: technical and managerial guidelines for catchment scale management. Mine water and the environment, 23, 2–80.

7 Figure and table captions

Figure 1 a) Simplified geological map (simplified from BRGM, Info Terre website); b) Map of the study area showing the main mining sites and the sampling stations (current stream sediments sampling stations : numbers represent stations on the main stream and AFx represents stations on the tributaries (AF1 Ravin des Bernes River, AF2 Richaldon River, AF3 Galeizon River, AF4 Grabieux River, AF5 Alzon River, AF6 Avène River, AF7 Salindrenque River, AF8 Aiguesmortes River, AF9 Amous River, AF10 Ourne River); Locations of sampling stations are available in supplementary information, SI Table 1

Figure 2 Enrichment Factors (EF) of As, Pb, Hg, Cd, Zn, Tl and Sb in sediments of the archive (◆) and in current stream sediments (●) sampled on November 2011 at the station 25. Datation from Dezileau et al., 2013 and Dezileau et al., in review

Figure 3 Temporal evolution of a) EF Tl vs. EF As and b) EF Pb vs. EF Zn in the sedimentary archive and in the current stream sediment sampled at the station 25 in 2011

Figure 4 Enrichment Factors (EF) of As, Cd, Hg, Pb, Sb, Tl and Zn in sediments sampled during the most complete campaign (December 6-7, 2012). EF are represented using bar charts for sediments of the main stream and a dot with EF value for sediments of the tributaries

Figure 5 a) $\delta^{66}Zn$ (‰) variations in the sedimentary archive and b) $\delta^{66}Zn$ (‰) in current stream sediments of the campaign of November 2011

Figure 6 Chemical partitioning of Cd, Zn, Pb, Tl, As and Sb in sediments of the archive between operationally defined fractions F1, F2, F3 and F4, expressed as percentage of total metal content and enrichment factor EF values. F1: exchangeable and bound to carbonates, F2: bound to Fe/Mn oxyhydroxides, F3: bound to organic matter (OM) and sulfides and F4: residual fraction

Table 1 Gardon River tributaries characteristics. Station number AFx indicate the sampling station location on the tributaries

Table 2 Metal/aluminum ratios in samples examined for geochemical background determination

Table 3 Spearman's correlation matrix for the metal(loid)/aluminum ratios in the sedimentary archive

Table 4 Spearman's correlation matrix for the metal(loid)/aluminum ratios in current stream sediments : the left lower part is correlation coefficient (R^2) for the Gardon of Ales River; the right upper part is for the Gardon of Anduze River

Table 5 Chemical partitioning of Cd, Zn, Pb, Tl, As and Sb in current stream sediments between operationally defined fractions F1, F2, F3 and F4, expressed as percentage of total metal content and enrichment factor EF values. F1: exchangeable and bound to carbonates, F2: bound to Fe/Mn oxyhydroxides, F3: bound to organic matter (OM) and sulfides and F4: residual fraction

8 Supplementary information

SI Table 1 Sampling station locations

SI Table 2 $\delta^{66}Zn$ values in the sedimentary archive relative to the standards "JMC Lyon 3-0749-L" and "IRMM 3702"

SI Table 3 $\delta^{66}Zn$ values in current stream sediments of the campaign of November 2011 relative to the standards "JMC Lyon 3-0749-L" and "IRMM 3702"

SI Table 4 As, Cd, Hg, Pb, Sb, Tl and Zn concentrations (in $\mu g.g^{-1}$) and enrichment factors in the sedimentary archive

SI Table 5 As, Cd, Hg, Pb, Sb, Tl and Zn concentrations (in $\mu g.g^{-1}$) and enrichment factors of the whole dataset of current stream sediments

Tributaries	Station number	Characteristics
Ravin des Bernes River	AF1	Former Sb mining site drainage
Richaldon River	AF2	Former Sb, Pb, Zn mining site drainage
Galeizon River	AF3	Unimpacted
Grabieux River	AF4	Urban tributary with former coal, pyrite, Pb and Zn mining sites drainage
Alzon River	AF5	Former pyrite, Pb and Zn mining sites drainage
Avene River	AF6	Former pyrite, Pb and Zn mining sites drainage and industrial activity discharge
Salindrenque River	AF7	Unimpacted
Aiguesmortes River	AF8	Former Pb and Zn mining sites drainage
Amous River	AF9	Former Pb and Zn mining sites drainage
Ourne River	AF10	Former Pb and Zn mining sites drainage

		As/Al 10^3	Cd/Al 10^3	Hg/Al 10^3	Pb/Al 10^3	Sb/Al 10^3	Tl/Al 10^3	Zn/Al 10^3
Sedimentary archive : Bottom layers GE1 to GE6 (n=7)	Mean	0.42	0.0036	0.0003	0.61	0.052	0.016	1.45
	Standard error	0.04	0.0005	0.0001	0.04	0.005	0.001	0.08
Upper Continental Crust		0.02[a]	0.0012[a]	0.0007[b]	0.25[a]	0.002[a]	0.009[a]	0.88[a]

[a] Taylor and Mc Lennan 1995 ; [b] Wedepohl 1995

	Zn/Al	As/Al	Cd/Al	Sb/Al	Tl/Al	Pb/Al	Hg/Al
Zn/Al							
As/Al	**0.71*** **						
Cd/Al	**0.87*** **	**0.71*** **					
Sb/Al	**0.69*** **	**0.62*** **	**0.75*** **				
Tl/Al	**0.85*** **	**0.72*** **	**0.73*** **	**0.60*** **			
Pb/Al	**0.87*** **	**0.77*** **	**0.81*** **	**0.63*** **	**0.85*** **		
Hg/Al	**0.69*** **	**0.56*** **	**0.77*** **	**0.66*** **	**0.70*** **	**0.61*** **	

***p-value <0.0001

	Zn/Al	As/Al	Cd/Al	Sb/Al	Tl/Al	Pb/Al	Hg/Al
Zn/Al		**0.51****	**0.93****	0.17	**0.23***	**0.65****	**0.54****
As/Al	**0.47***		**0.48****	0.07	**0.33***	**0.65****	**0.31***
Cd/Al	**0.90****	**0.44***		0.15	**0.25***	**0.67****	**0.54****
Sb/Al	0.00	0.04	0.00		0.00	0.04	0.02
Tl/Al	**0.56****	**0.42***	**0.49***	0.08		**0.57****	**0.39***
Pb/Al	**0.70****	**0.58****	**0.58****	0.00	**0.58****		**0.77****
Hg/Al	0.11	**0.57***	0.10	0.15	**0.49***	**0.69***	

*p-value<0.05

**p-value <0.001

	Gardon of Ales River				*Gardon of Anduze River*				*Gardon River*
Station number	1	3	9	11	13	15	22	23	24
Cadmium									
F1	32	40	48	38	25	27	44	62	53
F2	20	16	31	10	16	17	7	11	21
F3	16	11	9	10	17	13	25	11	10
F4	33	33	12	41	42	43	24	16	16
F1+F2+F3	67	67	88	59	58	57	76	84	84
EF	1.4	1.3	5.3	4.6	1.2	1.2	1.8	2.3	4.0
Zinc									
F1	9	11	37	12	6	8	21	22	23
F2	6	6	15	7	5	6	10	12	17
F3	13	12	13	6	13	13	20	22	14
F4	72	71	35	75	75	74	49	44	46
F1+F2+F3	28	29	65	25	25	26	51	56	54
EF	1.6	1.3	3.4	4.9	1.1	1.2	1.5	1.9	2.5
Lead									
F1	13	7	8	3	4	9	14	20	5
F2	28	33	43	19	18	30	34	31	35
F3	5	5	8	4	3	4	6	4	5
F4	54	54	41	74	75	56	46	45	55
F1+F2+F3	46	46	59	26	25	44	54	55	45
EF	1.0	1.0	1.7	4.2	1.0	0.9	2.0	3.2	3.6
Thallium									
F1	1	1	9	4	1	1	1	1	2
F2	6	3	29	17	5	2	7	6	14
F3	1	1	5	4	2	1	4	4	4
F4	92	96	56	75	92	97	89	89	79
F1+F2+F3	8	4	44	25	8	3	11	11	21
EF	0.7	0.6	1.8	1.9	1.0	0.7	1.2	1.5	2.1
Arsenic									
F1	1	2	10	1	1	2	2	2	2
F2	3	8	8	2	8	10	18	13	16
F3	2	4	3	1	3	3	4	3	4
F4	93	86	79	96	87	85	75	82	78
F1+F2+F3	7	14	21	4	13	15	25	18	22
EF	1.0	0.7	1.1	2.4	1.3	1.9	2.0	2.3	2.2
Antimony									
F1	0	0	2	0	1	0	1	1	1
F2	1	2	1	1	2	1	2	2	3
F3	0	1	1	0	0	0	1	0	1
F4	98	97	96	98	97	99	97	97	95
F1+F2+F3	2	3	4	2	3	1	3	3	5
EF	1.6	7.4	3.6	5.7	0.9	0.7	1.0	1.5	1.4

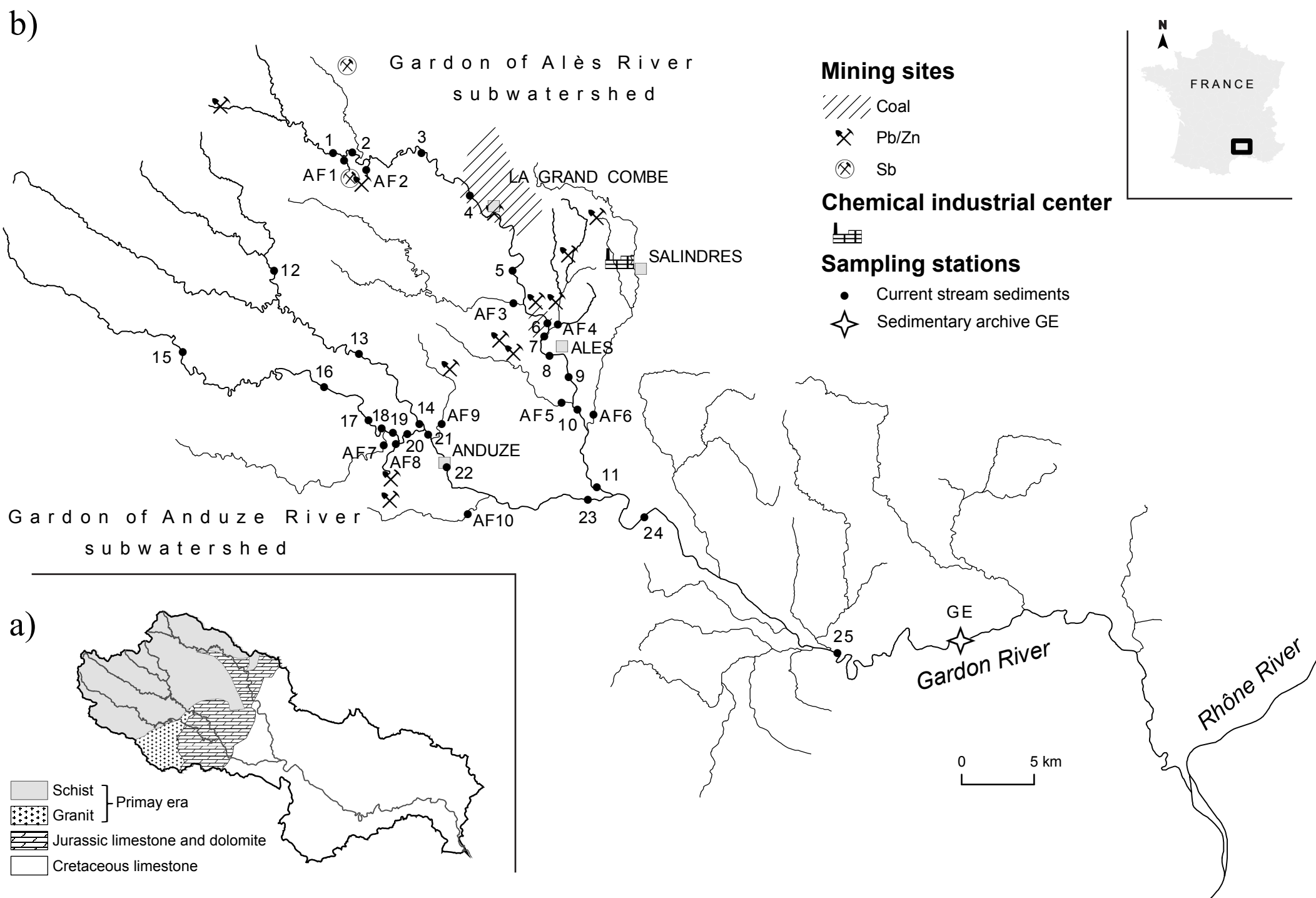
b)
Gardon of Alès River subwatershed
Gardon of Anduze River subwatershed
LA GRAND COMBE
SALINDRES
ALES
ANDUZE
AF1
AF2
AF3
AF4
AF5
AF6
AF7
AF8
AF9
AF10
1
2
3
4
5
6
7
8
9
10
11
12
13
14
15
16
17
18
19
20
21
22
23
24
25
GE
Gardon River
Rhône River
0
5 km
N
FRANCE
Mining sites
Coal
Pb/Zn
Sb
Chemical industrial center
Sampling stations
Current stream sediments
Sedimentary archive GE
a)
Schist
Granit
Primay era
Jurassic limestone and dolomite
Cretaceous limestone

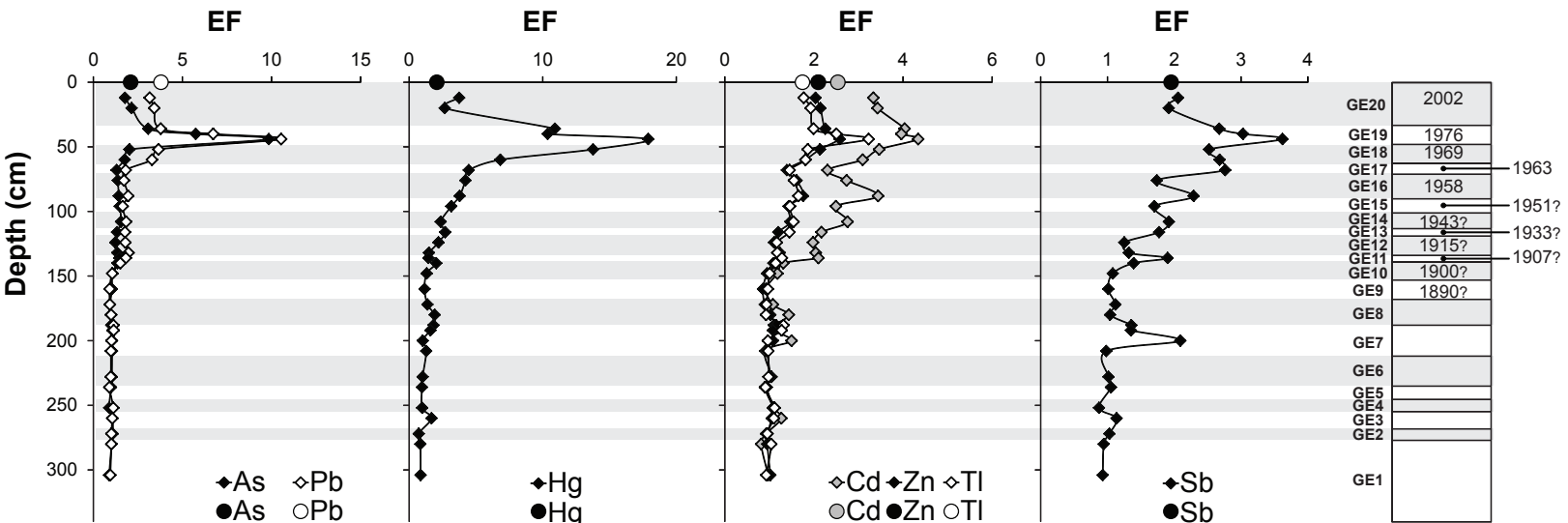
EF
EF
EF
EF
Depth (cm)
0
50
100
150
200
250
300
As
Pb
As
Pb
Hg
Hg
Cd
Zn
Tl
Cd
Zn
Tl
Sb
Sb
GE20
2002
GE19
1976
GE18
1969
GE17
1963
GE16
1958
GE15
1951?
GE14
1943?
GE13
1933?
GE12
1915?
GE11
1907?
GE10
1900?
GE9
1890?
GE8
GE7
GE6
GE5
GE4
GE3
GE2
GE1

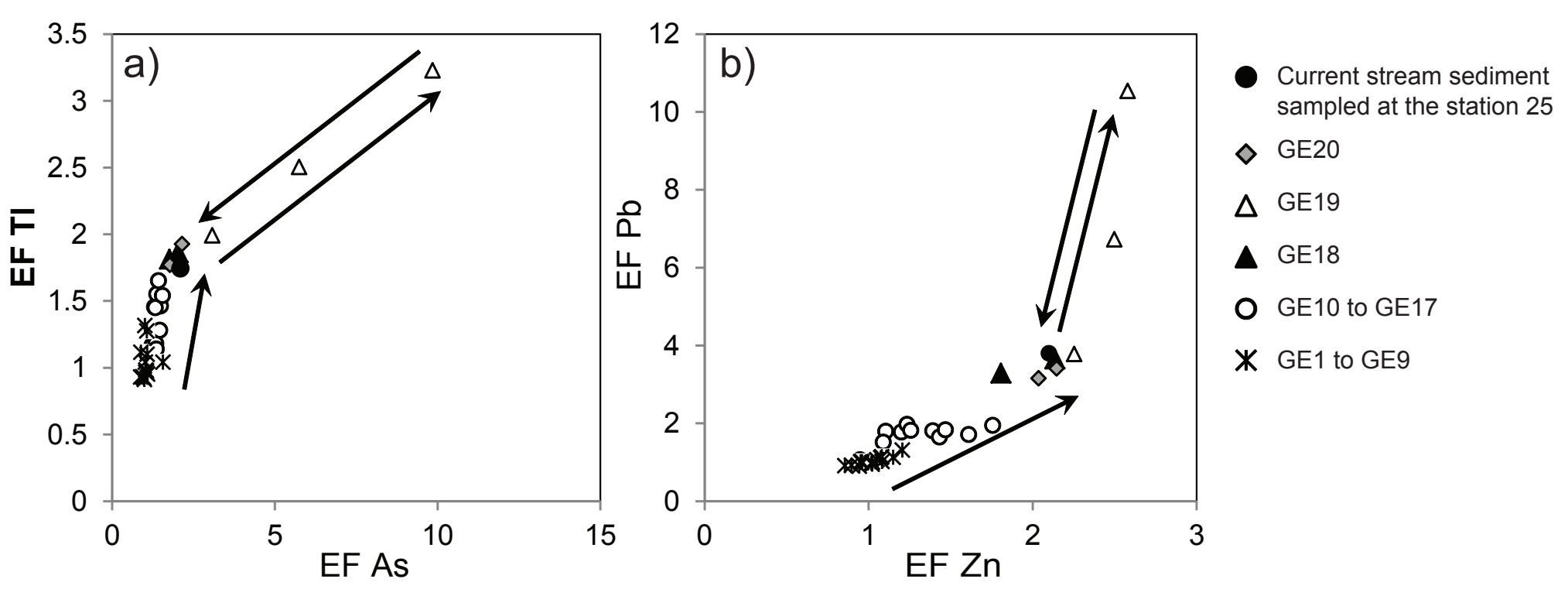
a)
b)
EF Tl
EF As
EF Pb
EF Zn
0
0.5
1
1.5
2
2.5
3
3.5
0
5
10
15
0
2
4
6
8
10
12
0
1
2
3
Current stream sediment sampled at the station 25
GE20
GE19
GE18
GE10 to GE17
GE1 to GE9

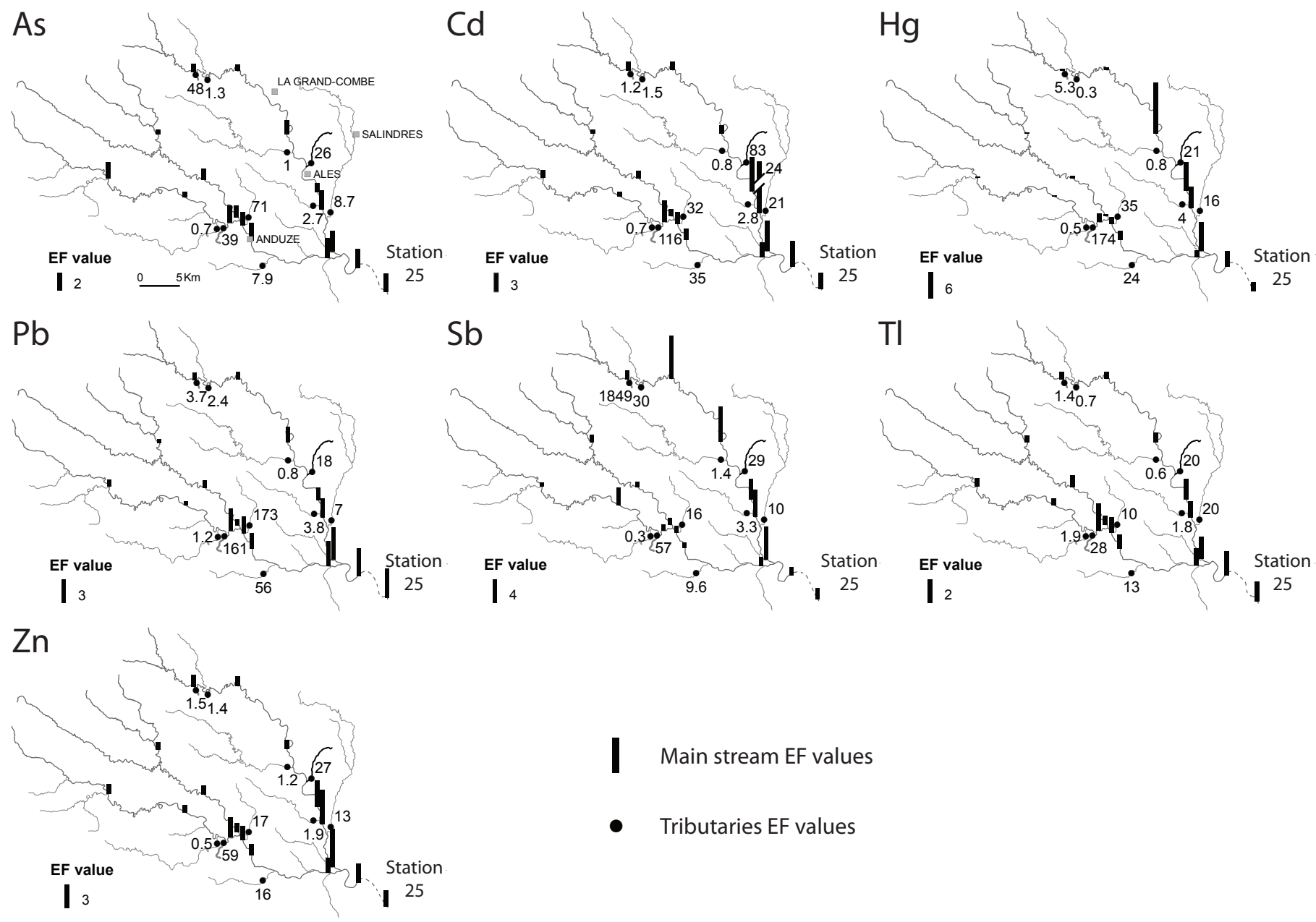
As
LA GRAND-COMBE
SALINDRES
ALES
ANDUZE
48
1.3
1
26
8.7
2.7
71
0.7
39
7.9
EF value
2
0 5Km
Station 25
Cd
1.2
1.5
0.8
83
24
21
2.8
32
0.7
116
35
EF value
3
Station 25
Hg
5.3
0.3
0.8
21
16
4
35
0.5
174
24
EF value
6
Station 25
Pb
3.7
2.4
0.8
18
7
3.8
173
1.2
161
56
EF value
3
Station 25
Sb
1849
30
1.4
29
16
0.3
57
3.3
10
9.6
EF value
4
Station 25
Tl
1.4
0.7
0.6
20
10
1.9
28
1.8
20
13
EF value
2
Station 25
Zn
1.5
1.4
1.2
27
13
1.9
17
0.5
59
16
EF value
3
Station 25
Main stream EF values
Tributaries EF values

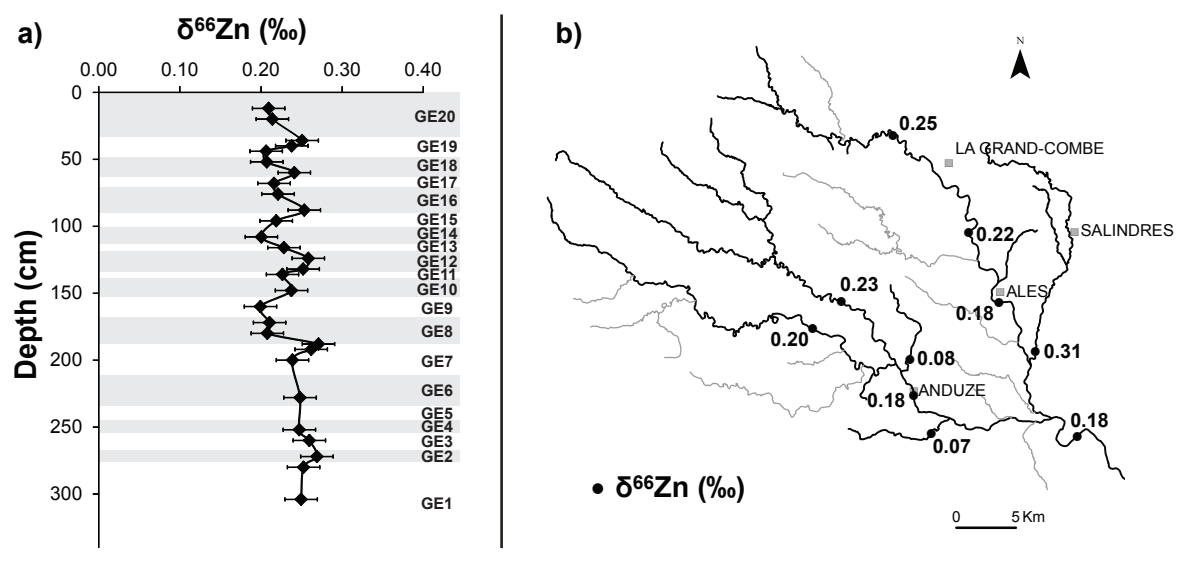
a)
δ66Zn (‰)
0.00
0.10
0.20
0.30
0.40
Depth (cm)
0
50
100
150
200
250
300
GE20
GE19
GE18
GE17
GE16
GE15
GE14
GE13
GE12
GE11
GE10
GE9
GE8
GE7
GE6
GE5
GE4
GE3
GE2
GE1
b)
N
LA GRAND-COMBE
SALINDRES
ALES
ANDUZE
0.25
0.22
0.23
0.18
0.20
0.08
0.31
0.18
0.18
0.07
• δ66Zn (‰)
0
5 Km

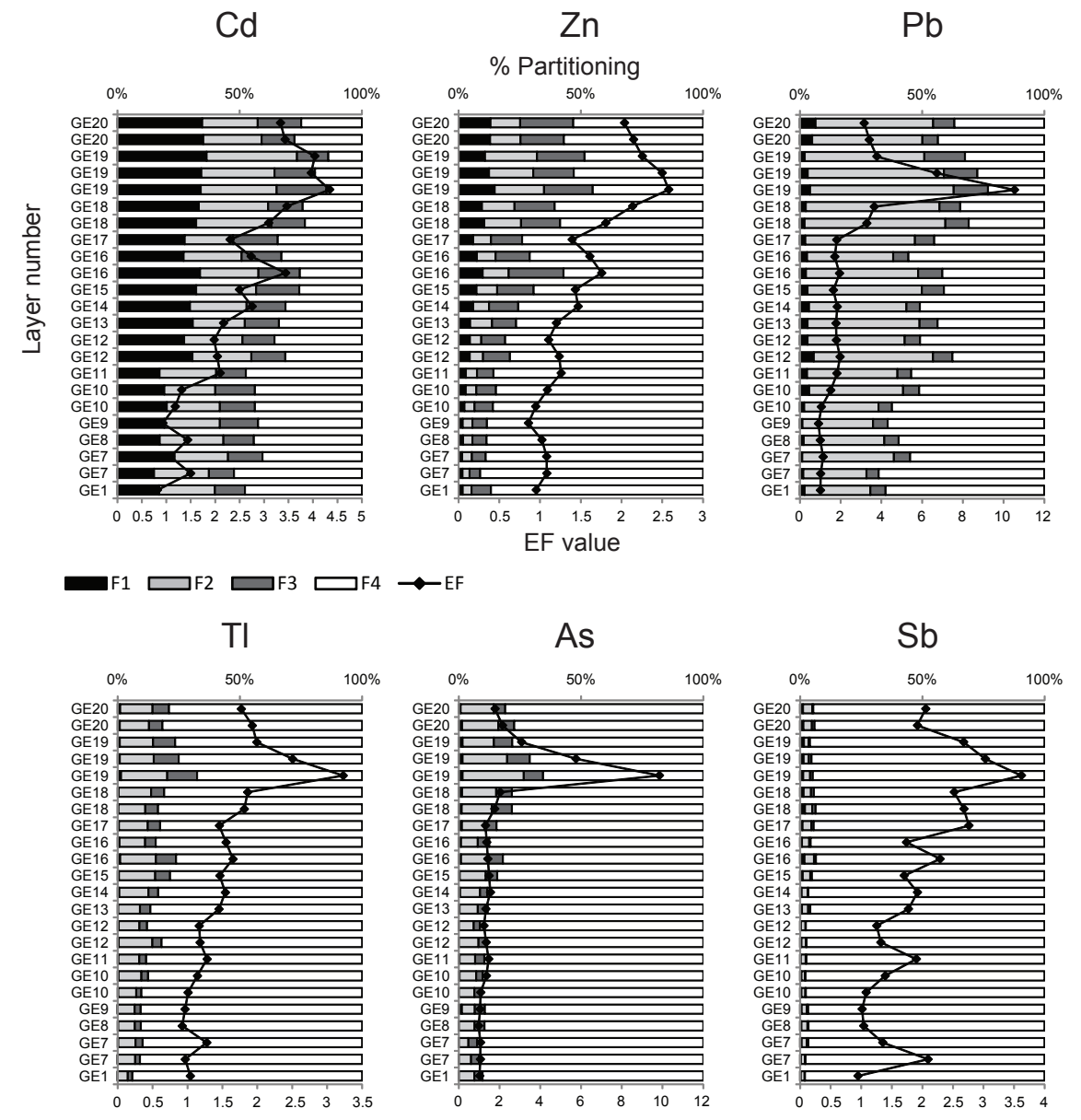
Cd
Zn
Pb
% Partitioning
0%
50%
100%
Layer number
GE20
GE19
GE18
GE17
GE16
GE15
GE14
GE13
GE12
GE11
GE10
GE9
GE8
GE7
GE1
EF value
F1
F2
F3
F4
EF
Tl
As
Sb

	Station	Longitude	Latitude
Main stream sediments	1	3.9015	44.2477
	2	3.9138	44.2474
	3	3.9724	44.2478
	3	3.9148	44.1236
	4	4.0137	44.2208
	5	4.0493	44.1736
	6	4.0783	44.1403
	7	4.0754	44.1322
	8	4.0795	44.1202
	9	4.0956	44.1066
	10	4.1026	44.0863
	11	4.1180	44.0374
	12	3.8429	44.1763
	14	3.9661	44.0794
	15	3.7626	44.1267
	16	3.8844	44.1034
	17	3.9221	44.0822
	18	3.9333	44.0771
	19	3.9429	44.0743
	20	3.9554	44.0731
	21	3.9735	44.0726
	22	3.9886	44.0521
	23	4.1101	44.0302
	24	4.1585	44.0182
	25	4.3221	43.9309
Tributary sediments	AF1	3.9054	44.2439
	AF2	3.9241	44.2381
	AF3	4.0493	44.1531
	AF4	4.0874	44.1394
	AF5	4.0892	44.0907
	AF6	4.1166	44.0829
	AF7	3.9348	44.0663
	AF8	3.9451	44.0669
	AF9	3.9854	44.0790
	AF10	4.0062	44.0226
Sedimentary archive	GE	4.4285	43.9369

Sampling depth[a] (cm)	$\delta^{66}Zn_{JMC\ 3\text{-}0749\text{-}L}$	$\delta^{66}Zn_{IRMM\ 3702}$
12	0.21	-0.08
20	0.21	-0.08
36	0.25	-0.04
40	0.24	-0.05
44	0.21	-0.08
52	0.21	-0.08
60	0.24	-0.05
68	0.22	-0.07
76	0.22	-0.07
88	0.25	-0.04
96	0.22	-0.07
108	0.20	-0.09
116	0.23	-0.06
124	0.26	-0.03
132	0.25	-0.04
136	0.23	-0.06
148	0.24	-0.05
160	0.20	-0.09
172	0.21	-0.08
180	0.21	-0.08
188	0.27	-0.02
192	0.26	-0.03
200	0.24	-0.05
228	0.25	-0.04
236	0.25	-0.04
252	0.25	-0.04
260	0.26	-0.03
272	0.27	-0.02
280	0.25	-0.04
304	0.25	-0.04

[a]mesured from the top of the terrace

Station number	$\delta^{66}Zn_{JMC\ 3\text{-}0749\text{-}L}$	$\delta^{66}Zn_{IRMM\ 3702}$
3	0.25	-0.04
5	0.22	-0.07
8	0.18	-0.11
13	0.23	-0.06
16	0.20	-0.09
22	0.18	-0.11
24	0.18	-0.11
AF6	0.31	0.02
AF9	0.08	-0.21
AF10	0.07	-0.22

Sampling depth[a] (cm)	As		Cd		Hg		Pb		Sb		Tl		Zn		Layer number	Dating
	µg.g^{-1}	EF	µg.g^{-1}	EF	µg.g^{-1}	EF	µg.g^{-1}	EF	µg.g^{-1}	EF	µg.g^{-1}	EF	µg.g^{-1}	EF		
12	33.2	1.8	0.53	3.3	0.053	3.7	84.8	3.2	4.78	2.1	1.26	1.8	130.7	2.0	GE20	2002
20	46.4	2.1	0.63	3.4	0.043	2.7	106.0	3.4	5.16	1.9	1.59	1.9	159.4	2.1		
36	84.7	3.1	0.95	4.0	0.225	10.9	253.7	3.8	9.14	2.7	2.09	2.0	212.8	2.3	GE19	1976
40	165.2	5.7	0.97	4.0	0.223	10.4	471.3	6.7	10.82	3.0	2.74	2.5	246.2	2.5		
44	275.8	9.8	1.04	4.3	0.376	17.9	720.0	10.5	12.60	3.6	3.45	3.2	247.9	2.6		
52	59.2	2.0	0.86	3.5	0.301	13.8	153.2	3.7	9.15	2.5	2.07	1.9	214.0	2.1	GE18	1969
60	53.1	1.8	0.80	3.1	0.155	6.8	142.6	3.3	10.05	2.7	2.09	1.8	187.2	1.8		
68	39.3	1.3	0.59	2.3	0.101	4.5	78.1	1.8	10.32	2.8	1.67	1.5	143.7	1.4	GE17	1963
76	30.7	1.4	0.52	2.7	0.071	4.2	55.1	1.7	4.84	1.7	1.33	1.6	123.8	1.6	GE16	1958
88	34.9	1.4	0.72	3.4	0.069	3.8	68.5	1.9	6.97	2.3	1.54	1.7	147.5	1.8		
96	47.0	1.5	0.67	2.5	0.075	3.2	74.7	1.6	6.69	1.7	1.76	1.5	155.4	1.4	GE15	1951?
108	38.4	1.5	0.58	2.8	0.044	2.4	65.3	1.8	5.91	1.9	1.46	1.5	124.8	1.5	GE14	1943?
116	38.4	1.3	0.53	2.2	0.058	2.7	73.5	1.8	6.35	1.8	1.60	1.5	118.8	1.2	GE13	1933?
124	31.9	1.2	0.44	2.0	0.043	2.2	66.7	1.8	4.03	1.3	1.15	1.2	98.2	1.1	GE12	1915?
132	43.5	1.3	0.56	2.0	0.036	1.5	91.8	2.0	5.32	1.3	1.46	1.2	137.5	1.2		
136	37.2	1.5	0.45	2.1	0.028	1.5	66.3	1.8	5.99	1.9	1.24	1.3	109.5	1.3	GE11	1907?
140	34.3	1.4	0.28	1.3	0.039	2.0	55.0	1.5	4.37	1.4	1.10	1.1	94.5	1.1	GE10	1900?
148	27.6	1.1	0.26	1.2	0.025	1.3	39.3	1.1	3.46	1.1	0.99	1.0	83.8	0.9		
160	30.4	1.0	0.23	0.9	0.025	1.2	38.3	0.9	3.68	1.0	1.07	1.0	85.8	0.9	GE9	1890?
172	31.5	0.9	0.31	1.1	0.035	1.4	44.7	0.9	4.68	1.1	1.19	0.9	103.3	0.9	GE8	n.d.
180	31.8	1.0	0.40	1.4	0.047	1.9	46.9	1.0	4.22	1.0	1.15	0.9	114.7	1.0		
188	35.5	1.0	0.33	1.1	0.048	1.8	57.3	1.1	5.96	1.4	1.77	1.3	139.6	1.1	GE7	n.d.
192	37.8	1.1	0.33	1.1	0.043	1.6	58.1	1.1	5.97	1.4	1.73	1.3	131.7	1.1		
200	29.0	1.1	0.35	1.5	0.021	1.0	40.3	1.0	7.16	2.1	1.02	1.0	102.3	1.1		
208	36.7	1.0	0.27	0.9	0.034	1.3	49.5	1.0	4.27	1.0	1.30	1.0	114.8	1.0		
228	32.7	1.0	0.28	1.0	0.024	1.0	44.3	1.0	3.99	1.0	1.18	1.0	110.2	1.0	GE6	n.d.
236	32.0	1.0	0.25	0.9	0.023	1.0	41.8	0.9	4.22	1.1	1.12	0.9	104.6	0.9	GE5	n.d.
252	22.5	0.9	0.24	1.1	0.019	1.0	40.6	1.1	2.75	0.9	1.08	1.1	93.5	1.1	GE4	n.d.
260	29.4	1.1	0.30	1.3	0.034	1.7	41.7	1.1	3.87	1.1	1.15	1.1	98.9	1.1	GE3	n.d.
272	33.8	1.1	0.25	0.9	0.017	0.7	45.0	1.0	3.97	1.0	1.13	1.0	102.2	1.0	GE2	n.d.
280	28.9	1.0	0.20	0.8	0.018	0.8	41.0	1.0	3.32	0.9	1.12	1.0	92.2	1.0	GE1	n.d.
304	25.2	0.9	0.24	1.0	0.018	0.9	38.9	0.9	3.30	0.9	1.01	0.9	100.1	1.0		

[a]mesured from the top of the terrace

n.d. not determined

Station number	As		Cd		Hg		Pb		Sb		Tl		Zn		Hydrological conditions	Sampling date	River
	µg.g^{-1}	EF	µg.g^{-1}	EF	µg.g^{-1}	EF	µg.g^{-1}	EF	µg.g^{-1}	EF	µg.g^{-1}	EF	µg.g^{-1}	EF			
1	27.5	1.0	0.34	1.4	0.009	0.4	40.1	1.0	5.58	1.6	0.72	0.7	153.5	1.6	Low flow	December 6-7, 2012	
2	24.6	0.9	0.63	2.8	n.d.	n.d.	48.3	1.3	19.97	6.1	0.62	0.6	172.9	1.9	High flow	March 17, 2011	
3	26.0	0.8	0.37	1.4	n.d.	n.d.	45.1	1.0	51.72	13.4	0.72	0.6	142.6	1.3	Low flow	March 10, 2011	
	24.8	0.6	0.29	0.8	0.033	1.1	54.7	0.9	29.42	5.7	0.97	0.6	152.4	1.1	High flow	November 7, 2011	
	21.9	0.7	0.33	1.3	0.011	0.5	41.0	1.0	27.22	7.4	0.67	0.6	127.1	1.3	Low flow	December 6-7, 2012	
4	20.5	0.8	0.26	1.3	n.d.	n.d.	26.0	0.7	19.41	6.4	0.64	0.7	82.5	1.0	Low flow	March 10, 2011	
5	20.6	0.7	0.28	1.2	n.d.	n.d.	36.0	0.9	7.85	2.3	0.70	0.7	82.2	0.9	Low flow	March 10, 2011	
	21.8	0.9	0.20	0.9	0.048	2.5	51.1	1.4	12.38	3.9	0.71	0.7	85.3	1.0	High flow	November 7, 2011	
	42.3	1.6	0.28	1.3	0.227	11.6	76.2	2.0	19.68	6.1	0.84	0.8	105.0	1.2	Low flow	December 6-7, 2012	Gardon of Ales River
6	17.4	0.6	0.59	2.5	n.d.	n.d.	67.2	1.7	4.93	1.4	1.00	1.0	194.5	2.1	High flow	March 17, 2011	
7	34.9	1.5	1.13	5.7	n.d.	n.d.	83.1	2.5	13.48	4.7	1.38	1.6	323.0	4.1	High flow	November 16, 2010	
8	29.8	1.2	0.55	2.6	0.092	5.0	58.7	1.7	8.15	2.7	1.53	1.6	192.6	2.3	High flow	November 7, 2011	
9	51.8	3.2	0.92	6.8	n.d.	n.d.	168.3	7.3	14.90	7.5	1.06	1.7	338.3	6.2	Low flow	March 10, 2011	
	24.2	1.1	1.02	5.3	0.112	6.6	54.3	1.7	10.10	3.6	1.56	1.8	265.2	3.4	Low flow	December 6-7, 2012	
10	33.5	2.2	3.11	23.7	0.058	5.0	54.3	2.4	8.92	4.6	0.81	1.4	235.4	4.4	Low flow	December 6-7, 2012	
11	13.3	0.8	0.55	4.0	0.012	1.0	34.4	1.5	4.25	2.1	0.70	1.1	167.6	3.0	Low flow	October 10, 2011	
	40.5	2.4	0.67	4.6	0.084	6.6	102.2	4.2	11.99	5.7	1.25	1.9	284.2	4.9	Low flow	December 6-7, 2012	
12	16.8	0.6	0.16	0.7	0.005	0.2	20.7	0.5	4.78	1.3	0.63	0.6	94.1	1.0	Low flow	December 6-7, 2012	
13	26.5	1.2	0.19	1.0	0.005	0.3	23.0	0.7	2.87	1.1	0.61	0.7	83.3	1.1	Low flow	October 10, 2011	
	31.9	1.2	0.21	1.0	0.005	0.2	28.7	0.8	2.88	0.9	0.60	0.6	99.9	1.1	High flow	November 7, 2011	
	29.4	1.3	0.23	1.2	0.009	0.5	31.1	1.0	2.47	0.9	0.88	1.0	87.1	1.1	Low flow	December 6-7, 2012	
14	20.6	1.3	0.15	1.1	0.005	0.4	18.6	0.8	2.31	1.2	0.47	0.8	62.3	1.2	Low flow	December 6-7, 2012	
15	57.5	1.9	0.31	1.2	0.005	0.2	39.4	0.9	2.60	0.7	0.80	0.7	130.0	1.2	Low flow	December 6-7, 2012	
16	27.0	1.0	0.28	1.2	0.013	0.6	59.2	1.5	0.97	0.3	0.87	0.9	121.6	1.3	High flow	November 7, 2011	
	19.3	0.6	0.19	0.7	0.007	0.3	24.0	0.6	11.42	3.0	0.67	0.6	98.7	1.0	Low flow	December 6-7, 2012	
17	47.7	2.1	0.11	0.6	0.005	0.3	35.0	1.1	1.34	0.5	1.17	1.3	58.4	0.7	Low flow	October 10, 2011	Gardon of Anduze River
18	30.3	1.1	0.23	1.0	0.008	0.4	39.1	1.0	1.77	0.5	1.33	1.3	96.7	1.0	Low flow	October 10, 2011	
19	29.7	1.1	0.11	0.5	0.011	0.6	55.3	1.5	1.70	0.5	1.74	1.7	71.0	0.8	Low flow	October 10, 2011	
20	46.4	2.0	0.68	3.4	0.033	1.8	99.3	2.9	3.04	1.0	2.11	2.3	213.7	2.6	Low flow	December 6-7, 2012	
21	25.3	1.5	0.27	1.9	0.021	1.7	51.4	2.2	2.46	1.2	0.83	1.3	106.0	1.9	Low flow	December 6-7, 2012	
22	35.2	1.7	0.39	2.3	0.044	2.9	68.9	2.4	2.09	0.8	1.05	1.4	109.1	1.6	Low flow	October 10, 2011	
	68.2	3.1	0.45	2.4	0.055	3.3	266.6	8.4	4.98	1.8	1.01	1.2	155.6	2.0	High flow	November 7, 2011	
	45.8	2.0	0.34	1.8	0.036	2.1	65.4	2.0	2.69	1.0	1.04	1.2	115.1	1.5	Low flow	December 6-7, 2012	
23	58.0	3.3	0.20	1.3	0.087	6.5	90.4	3.6	2.32	1.1	0.89	1.3	118.6	1.9	Low flow	October 10, 2011	
	45.5	2.3	0.39	2.3	0.023	1.5	91.7	3.2	3.73	1.5	1.14	1.5	132.6	1.9	Low flow	December 6-7, 2012	
24	52.9	2.3	0.27	1.4	0.024	1.4	120.4	3.7	3.76	1.3	1.23	1.4	159.7	2.0	Low flow	October 10, 2011	Gardon River downstream from the confluence of the Gardon of Anduze and Ales Rivers
	31.5	1.2	0.36	1.7	0.024	1.2	87.4	2.4	1.94	0.6	1.10	1.1	147.9	1.7	High flow	November 7, 2011	
	44.6	2.2	0.70	4.0	0.053	3.5	106.2	3.6	3.69	1.4	1.62	2.1	178.3	2.5	Low flow	December 6-7, 2012	
25	43.9	2.1	0.45	2.5	0.033	2.1	114.4	3.8	5.10	2.0	1.40	1.7	151.3	2.1	High flow	November 7, 2011	
AF1	1461.0	48.4	0.30	1.2	0.120	5.3	160.6	3.7	6942.15	#####	1.56	1.4	157.8	1.5	Low flow	December 6-7, 2012	
AF2	155.3	3.8	0.61	1.7	n.d.	n.d.	312.1	5.3	132.50	25.8	1.01	0.6	198.4	1.4	High flow	March 17, 2011	
	47.7	1.3	0.46	1.5	0.009	0.3	124.0	2.4	133.99	30.5	0.93	0.7	167.5	1.4	Low flow	December 6-7, 2012	
AF3	6.5	0.4	0.16	1.0	n.d.	n.d.	12.7	0.5	1.02	0.5	0.38	0.6	65.0	1.1	High flow	November 16, 2010	
	25.2	1.0	0.16	0.8	0.014	0.8	29.7	0.8	4.22	1.4	0.60	0.6	99.6	1.2	Low flow	December 6-7, 2012	
AF4	278.2	29.3	5.06	62.5	n.d.	n.d.	315.8	23.2	31.49	26.6	8.25	22.8	1197.0	36.7	High flow	November 16, 2010	Gardon of Ales River Tributaries
	240.6	26.0	6.58	83.5	0.143	20.6	238.0	17.9	33.79	29.4	7.05	20.0	855.0	26.9	Low flow	December 6-7, 2012	
AF5	34.4	2.7	0.31	2.8	0.039	4.0	69.8	3.8	5.33	3.3	0.90	1.8	85.5	1.9	Low flow	December 6-7, 2012	
AF6	50.1	6.6	1.21	18.9	n.d.	n.d.	70.8	6.5	9.01	9.6	3.89	13.5	314.0	12.1	High flow	November 16, 2010	
	45.9	4.2	1.48	16.0	0.191	23.5	69.4	4.5	6.27	4.7	7.33	17.8	354.5	9.5	High flow	November 7, 2011	
	55.3	8.7	1.15	21.3	0.074	15.7	63.4	7.0	7.97	10.1	4.91	20.4	288.0	13.3	Low flow	December 6-7, 2012	
AF7	5.4	0.2	0.08	0.3	0.013	0.6	49.4	1.2	0.10	0.0	1.90	1.8	69.0	0.7	Low flow	October 10, 2011	
	15.9	0.7	0.14	0.7	0.009	0.5	40.3	1.2	0.86	0.3	1.68	1.9	42.7	0.5	Low flow	December 6-7, 2012	
AF8	216.7	38.5	5.56	116.1	0.733	173.9	1295.4	160.5	39.91	57.1	5.99	27.9	1148.1	59.5	Low flow	December 6-7, 2012	
AF9	691.8	47.5	2.57	20.8	0.372	34.1	3957.7	189.5	4.59	2.5	4.41	7.9	763.9	15.3	Low flow	October 10, 2011	Gardon of Anduze River Tributaries
	877.9	70.3	3.47	32.6	0.365	39.0	4475.5	249.8	30.59	19.7	4.61	9.7	926.5	21.6	High flow	November 7, 2011	
	833.0	70.6	3.20	31.8	0.313	35.4	2927.2	172.9	24.14	16.5	4.63	10.3	679.8	16.8	Low flow	December 6-7, 2012	
AF10	125.4	20.2	2.83	53.7	0.163	35.1	1021.9	115.0	14.66	19.1	5.25	22.2	576.6	27.1	High flow	November 7, 2011	
	70.7	7.9	2.68	35.2	0.159	23.8	712.6	55.7	10.65	9.6	4.29	12.6	493.9	16.1	Low flow	December 6-7, 2012	

n.d. not determined